

TR-O-0070

49

GaAs(001)パターン基板上でのGaAs/AlGaAs
多層膜の分子線エピタクシー中のファセット成長

武部 敏彦

1994. 3. 31

ATR光電波通信研究所

ATR Technical Report

報告題名 : GaAs(001)パターン基板上でのGaAs/AlGaAs多層膜の分子線エピタクシー中のファセット成長*

報告者 : 武部 敏彦

所属 : ATR光電波通信研究所 通信デバイス研究室

報告内容概要 :

【1】研究の動機

GaAs(001)パターン基板上のGaAs、AlGaAs、InGaAsの成長、及びそれに基づいたデバイス応用に関しては数多くの報告がある。特に、 $[\bar{1}10]$ 方向のストライプパターンを有する(001)基板上での分子線エピタクシー(MBE)中のファセット成長はよく研究されているが、(111)A側壁か(113)A側壁の場合に限られている。 $[110]$ 方向のストライプパターン上でのファセット成長についてもいくつかの報告があり、最近漸く $[100]$ 方向のストライプパターン上でのファセット成長についても報告が出始めている。

我々のグループでは(111)Aパターン基板上にMBEでGaAs/AlGaAs多層膜を成長する間に生じるファセットを系統的に研究してきた[#]。従って、パターン基板上での結晶成長をより深く理解するために、異なる方位のパターン基板上でのファセット成長を比較検討することは、基板表面特性の違い、ある側壁の基板面に対する相対的位置の違い、実効入射分子線フラックスの違い、等を考慮すると非常に意義深いことと考えられる。

本報告では、(001)基板上の異なる側壁傾斜角を有するストライプパターン上にMBEでGaAs/AlGaAs多層膜を成長する間に、側壁やストライプ間の交差点に生じるファセットを系統的に調べた。側壁傾斜角と関連付けてファセット発生の変化あるいは制御について詳細に論ずる。我々の知る限り、(001)基板上で側壁傾斜角を変化させたスト

ライブ上に成長させた報告、ストライプ間の交差点での成長の様子を論じた報告はこれまでにない。

【2】研究の成果

GaAs(001)基板上に $\text{HF} + \text{H}_2\text{O}_2 + \text{H}_2\text{O}$ エッチング液[※]による選択エッチングで、(111)A面関連、 $(\bar{1}\bar{1}\bar{1})$ B面関連、及び(010)面関連の側壁を有する $[\bar{1}\bar{1}0]$ 方向のストライプ、 $[110]$ 方向のストライプ、及び $[100]$ 方向のストライプを形成した。これらをそれぞれ、 $[\bar{1}\bar{1}0]$ ストライプ、 $[110]$ ストライプ、及び $[100]$ ストライプと名付ける。この上に、MBEでGaAs/AlGaAs多層膜を成長させ、成長中に生じるファセットを側壁傾斜角 θ と関連付けて調べた。結果は以下の様にまとめられる。

1. $[\bar{1}\bar{1}0]$ ストライプでは、(111)A及び(114)Aファセットが、 $[110]$ ストライプでは、 $(\bar{1}\bar{1}\bar{1})$ B及び $(\bar{1}\bar{1}\bar{3})$ Bファセットが、 $[100]$ ストライプでは、(031)、(011)、(045)、及び(013)ファセットが、 θ に応じて側壁上に発生し、元のストライプパターンを変形させた。
2. この中で、(114)A、 $(\bar{1}\bar{1}\bar{3})$ B、及び(013)ファセットは広い θ 範囲にわたって存在し、従って(001)パターン基板上で平坦で均一な側壁層を形成するのに重要な要素である。
3. 側壁上にファセットを生じさせず、元のストライプパターンを維持しながら成長させるには、 $[\bar{1}\bar{1}0]$ ストライプでは $10^\circ \geq \theta$ 、 $[110]$ ストライプでは $24^\circ \geq \theta \geq 20^\circ$ 、 $[100]$ ストライプでは $19^\circ \geq \theta$ に θ を制御する必要がある。
4. 一方、互いに直交する等価な $[100]$ と $[010]$ ストライプの(111)A関連交差点では(111)A関連ファセットが発生したが、 $(\bar{1}\bar{1}\bar{1})$ B関連交差点ではファセットは発生しなかった。
5. (111)Aパターン基板上でのファセット発生[#]との比較により、(114)A、 $(\bar{1}\bar{1}\bar{1})$ B、及び(110)ファセットが(111)Aと(001)パターン基板上に共通に生じることが明らかとなった。

以上

* 本報告は、本文中ではPaper IIと名付けられている。

ATR Technical Report 「GaAs(111)Aパターン基板上でのGaAs/AlGaAs多層膜の分子線エピタクシー中のファセット成長」(Paper I)。

※ ATR Technical Report 「GaAs選択エッチング用HF+H₂O₂+H₂O混合液の基本特性」。

目次

Abstract	1
1. Introduction	3
2. Experiment	3
3. Results and Discussion	4
1. $[\bar{1}10]$ stripe	4
2. $[110]$ stripe	6
3. $[100]$ stripe	8
4. Intersections of orthogonal stripes	10
5. Phenomena common to three stripe patterns	11
6. Comparison with $(111)A$ patterned substrates	12
4. Summary and Conclusion	13
ACKNOWLEDGMENTS	13
REFERENCES	14
FIGURE CAPTIONS	17
TABLE HEADINGS	19
Figure	20
Table	37

Facet Generation During Molecular Beam Epitaxy of GaAs/AlGaAs Multilayers on GaAs (001) Patterned Substrates

-Abstract-

Extra facet generation during molecular beam epitaxy of GaAs/AlGaAs multilayers on (001) GaAs substrates patterned with stripes running in the $[\bar{1}10]$, $[110]$, and $[100]$ directions and having various slopes, designated as “ $[\bar{1}10]$ stripe”, “ $[110]$ stripe”, and “ $[100]$ stripe”, respectively, has systematically been investigated for the first time. It has been confirmed that extra (111)A and (114)A facets generate on the $[\bar{1}10]$ stripes, extra $(\bar{1}11)$ B and $(\bar{1}13)$ B facets on the $[110]$ stripes, and extra (031), (011), (045), and (013) facets on the $[100]$ stripes, depending on the intersection angle θ of the sidewall and the substrate plane. Among them, the (114)A, $(\bar{1}13)$ B, and (013) facets are important because they persist over a wide range of θ and, therefore, play a detrimental role in forming flat and uniform sidewall layers on the (001) patterned substrates. It has been made clear that no extra facets generate on the sidewalls and flat and uniform layers maintaining the initial as-etched stripe patterns can be grown for the $[\bar{1}10]$ stripes with $10^\circ \geq \theta$, the $[110]$ stripes with $24^\circ \geq \theta \geq 20^\circ$, and the $[100]$ stripes with $19^\circ \geq \theta$. Extra (111)A-related facets have developed on the (111)A-related intersection of the equivalent $[100]$ and $[010]$ stripes, while no extra facets have developed on the $(\bar{1}11)$ B-related intersection.

Key words : gallium arsenide, aluminum gallium arsenide, patterned substrate,
molecular beam epitaxy, crystal facet.

1. Introduction

In the preceding paper, designated as Paper I, facet generation behavior during molecular beam epitaxy (MBE) of GaAs/AlGaAs multilayers on GaAs (111)A substrates patterned with ridge-type triangles was investigated. It is very profitable to compare these results with those on patterned substrates with other orientations for deeper understanding of crystal growth on nonplanar substrates because of the differences in the surface properties, the position of a sidewall relative to the substrate plane, and the incident effective molecular beam fluxes. In this respect, there are many papers published on crystal growth and microstructure formation on (001) patterned substrates and they provide useful information [1-21]. Almost of these papers have dealt with the growth on stripes running in the $[\bar{1}10]$ direction with the exact (111)A sidewall [1-5, 10, 11, 13, 15-17, 19] or the (113)A sidewall [6-9, 14]. Several papers have discussed the growth on stripes running in the [110] direction [1, 2, 4, 11, 12, 18, 19, 21] and very recently on stripes running in the [100] direction with the (010) sidewall [20]. To our knowledge, no papers have been published systematically studying growth on stripes with various sidewall slopes or on intersections of two stripes running in the orthogonal directions.

In the present paper, designated as Paper II, extra facet generation during MBE of GaAs/Al_{0.3}Ga_{0.7}As multilayers on the stripes running in the $[\bar{1}10]$, [110], and [100] directions with various slopes and their intersections on (001) substrates is investigated for the first time.

2. Experiment

Considering the two-fold rotational symmetry of the (001) surface, stripes running in the $[\bar{1}10]$, [110], and [100] directions with heights of 5 - 7 μm whose sidewalls are composed of (111)A-related, $(\bar{1}11)$ B-related, and (010)-related surfaces, respectively, were formed on the (001) substrates using photolithography and selective etching techniques. They are briefly designated as " $[\bar{1}10]$ stripe", "[110] stripe", and "[100] stripe", respectively. These stripes are schematically

shown with respect to the atomic configuration of the (001) surface in Figure 1. The [010] stripe is a mirror image of the [100] stripe with respect to the $(\bar{1}10)$ plane and has sidewall orientations equivalent to those of the [100] stripe. The intersection angle θ of the side wall and the (001) substrate plane was varied in the range of 54° to 9° for the $[\bar{1}10]$ stripe, of 57° to 9° for the [110] stripe, and of 89° to 9° for the [100] stripe using H_2O_2 -excess $\text{HF} + \text{H}_2\text{O}_2 + \text{H}_2\text{O}$ mixtures of various compositions [22]. These θ ranges include various low- and high-index planes for the sidewalls. The (001) patterned substrates were subjected to the same MBE growth runs as the (111)A patterned substrates discussed in Paper I: The (001) patterned substrates were chemically etched in an $\text{NH}_4\text{OH}:\text{H}_2\text{O}_2:\text{H}_2\text{O}=2:1:96$ (volume ratio) mixture and thermally treated at 700°C under an As_4 pressure of 4.0×10^{-5} Torr. Finally, five pairs of undoped $0.2 \mu\text{m}$ thick GaAs/ $0.2 \mu\text{m}$ thick $\text{Al}_{0.3}\text{Ga}_{0.7}\text{As}$ layers and an undoped $0.3 \mu\text{m}$ thick GaAs cap were successively grown by MBE on the (111)A patterned substrates at a substrate temperature of 620°C , an As_4 pressure of 3.3×10^{-5} Torr, a V/III flux ratio of 7.4 for GaAs and 6.2 for AlGaAs, and a substrate rotation speed of 60 rpm. The growth rate was $0.77 \mu\text{m/h}$ for GaAs and $1.10 \mu\text{m/h}$ for AlGaAs, corresponding to 0.76 and 1.08 monolayers/sec, respectively. The AlGaAs layers were used as "markers" in order to observe how the growth proceeded. The layers grown on the stripes have been closely examined by scanning electron microscopy (SEM) at an acceleration voltage of 10 kV and a probe current of 1 nA as shown in Figure 1. For a cross-sectional observation, the $(\bar{1}10)$ and (110) cleaved surfaces were stain-etched in an $\text{HF}:\text{H}_2\text{O}_2:\text{H}_2\text{O}=1:1:10$ (volume ratio) mixture to clearly reveal the GaAs/AlGaAs interfaces. No variations of the as-etched sidewall profile, growth rate, and after-growth surface morphology were confirmed across the whole sample ($20 \times 25 \text{ mm}^2$) for any of the samples investigated.

3. Results and Discussion

1. $[\bar{1}10]$ stripe

Figure 2 shows $(\bar{1}10)$ cross-sectional views of the as-etched profiles of the

(111)A-related sidewalls of the $[\bar{1}10]$ stripes with various values of θ . The surface index corresponding to each value of θ is also shown (within $\pm 2^\circ$). Figure 3 shows $(\bar{1}10)$ cross-sectional views of the corresponding grown layers. The brighter layers correspond to GaAs and the darker layers to AlGaAs. Generation of extra facets on the sidewalls is described as follows:

(a)-(g) For $\theta > 21^\circ$, extra (114)A and (111)A facets with $\theta_f = 21^\circ$ and 55° to the (001) substrate plane, respectively were clearly identified. As θ approached 21° , θ_f of the (114)A facet, the (114)A facet developed more towards the sidewall, while the (111)A facet receded towards the lower (001) substrate plane.

(h)-(i) For $\theta \leq 21^\circ$, both (114)A and (111)A facets disappeared and no extra facets generated, leading to a flat and uniform sidewall that maintained the initial as-etched profile.

Thus, the general rule of facet generation with respect to θ that a facet present for large θ vanishes once θ decreases below θ_f of the facet, demonstrated on the (111)A patterned substrates in Paper I, holds for the (114)A facet but not for the (111)A facet on the (001) patterned substrates.

The generation of the (114)A facet on the $[\bar{1}10]$ stripe has also been reported in the literature under different growth conditions but only for the exact (111)A [1, 2, 4, 5, 13, 16] and (113)A [6, 7, 14] sidewalls. Thus, it has been confirmed for the first time in the present study that the generation of the (114)A facet is a common feature independent of the sidewall orientation.

Figure 4 shows bird's eye views of the growth behavior of the (114)A facet with respect to θ . The surface morphology of the (114)A facet is identical with those reported in the literature [4, 6, 14] and does not change with θ . The development of the (114)A facet towards the sidewall with decreasing θ is also clearly observed. As was mentioned for the (111)A patterned substrates in Paper I, it seems to be caused by enhancement of the lateral growth due to the increase in the terrace width of microsteps formed on the as-etched sidewall. For $\theta \geq 48^\circ$, the layers grown on the sidewall clearly exhibited step structures composed of the equivalent (011)-related and (101)-related facets ((a)-(b)). Since these sidewalls

correspond to the (111)A planes misoriented by 1° to 7° towards the [001] direction, it is natural that the sidewall layers exhibited step structures identical with those of the layers grown on the planar (111)A substrates misoriented towards the [001] direction as shown in Paper I. The average interstep distance shortened from $1.5 \mu\text{m}$ to $0.5 \mu\text{m}$ as θ decreased from 54° to 48° . Figure 5(a) shows the magnified $(\bar{1}10)$ cross-sectional image corresponding to Figure 4(b). We observe giant steps with about $0.5 \mu\text{m}$ wide terraces and the corresponding Al composition variation (seen as a lateral gradation in the AlGaAs layers), which are identical with the step structures discussed in [23]. For $41^\circ \geq \theta \geq 21^\circ$, except for the (114)A facet, the surface morphology of the sidewall layers was poor and seemed to be dependent on θ (shown in (c)-(d); see also Figure 15 below). For $\theta \leq 21^\circ$, the sidewall layer maintained an excellent surface morphology, as observed in (f).

Table 1 summarizes the facet generation behavior for the $[\bar{1}10]$ stripe. In order to obtain flat and uniform layers on the sidewall that maintain the initial as-etched pattern, it is necessary to keep θ smaller than 21° . This result is close to that suggested in [6] under a higher growth temperature of 720°C and a lower V/III flux ratio of 1, which indicates that (114)A facet generation cannot be well controlled by the growth conditions. In contrast to the (001) triangles on (111)A substrates, the exponential thickness variation of the layers grown on the (001) substrate plane persists after flat and uniform layers on the sidewall are grown for $\theta \leq 21^\circ$ as shown in Figures 3(h) and 4(f). In order to obtain flat and uniform layers across the sidewall - substrate plane intersection, θ must actually be smaller than 10° . This point is critically important for device application, as will be discussed in the subsequent paper designated as Paper III, but has been ignored so far.

2. [110] stripe

Figure 6 shows (110) cross-sectional views of the as-etched profiles of the (111)B-related sidewalls of the [110] stripes with various values of θ . The $\text{HF} + \text{H}_2\text{O}_2 + \text{H}_2\text{O}$ mixtures used produce an inverted $(\bar{1}\bar{1}\bar{1})\text{A}$ -related mesa together with the normal $(\bar{1}11)\text{B}$ -related sidewall for large θ [22]. Figure 7 shows (110)

cross-sectional views of the corresponding grown layers. Generation of extra facets on the sidewalls is described as follows:

(a)-(c) For $\theta \geq 53^\circ$, an extra $(\bar{1}11)B$ facet with $\theta_f = 53^\circ$ was observed at the edge of the inverted mesa.

(d)-(g) For $53^\circ > \theta \geq 24^\circ$, the $(\bar{1}11)B$ facet disappeared and an extra $(\bar{1}13)B$ facet with $\theta_f = 24^\circ$ developed as θ decreased.

(h)-(j) For $24^\circ > \theta$, the $(\bar{1}13)B$ facet disappeared and no extra facets were observed.

The generation of the $(\bar{1}11)B$ facet on the $[110]$ stripe with an inverted mesa has also been reported in the literature under different growth conditions [1, 12, 18]. To our knowledge, the present study provided the first systematic data on the growth behavior for the $[110]$ stripes over a wide θ range.

Table 1 summarizes the facet generation behavior for the $[110]$ stripe. In order to obtain layers on the sidewall that maintain the initial as-etched pattern, it is necessary to keep θ smaller than 24° . In fact, taking the surface morphology of the sidewall layers into account, the usable θ range is further restricted as discussed below.

Figures 8 show bird's eye views of the growth behavior of the $(\bar{1}11)B$ facet with respect to θ . It should be noted that the layers grown on the sidewalls with θ around θ_f of the $(\bar{1}11)B$ plane exhibited a very rough surface morphology, whereas the $(\bar{1}11)B$ facet with a relatively smooth surface grew at the edge of the (001) surface without underlying $(\bar{1}11)B$ surfaces. The present growth conditions of high temperatures and high As_4 pressures probably did not match the growth on the $(\bar{1}11)B$ surface favoring high temperatures, low As_4 pressures, and low growth rates [24-31]. The round as-etched profiles of the sidewalls may be another source of generating such a faceted surface. As to the $(\bar{1}11)B$ facet, a lateral flow of excess Ga adatoms not incorporated on the initially formed $(\bar{1}11)B$ plane to the substrate plane resulted in the low growth rate in the $[\bar{1}11]B$ direction, hence the formation of the $(\bar{1}11)B$ facet with a relatively smooth surface. This will be discussed in Paper III.

Figure 9 shows bird's eye views of the growth behavior of the $(\bar{1}13)B$ facet with respect to θ . It is clearly observed in (a)-(c) that the $(\bar{1}13)B$ facet with a smooth surface grew towards the sidewall with the rough surface as θ decreased. The whole sidewall is expected to be covered with the smooth $(\bar{1}13)B$ facet for θ around 24° , θ_f of the $(\bar{1}13)B$ facet (not checked experimentally). The generation of the $(\bar{1}\bar{1}\bar{3})B$ facet has been reported in [32] in the lateral growth of GaAs on $(\bar{1}\bar{1}\bar{1})B$ patterned substrates by metalorganic MBE (MOMBE). The smooth surface was maintained after the $(\bar{1}13)B$ facet vanished for $\theta=20^\circ$ as shown in (d), but the surface morphology got worse again as θ decreased further. Consequently, the [110] stripes with flat and uniform sidewall layers maintaining the initial as-etched pattern can be obtained in the narrow θ range of 24° to (at least) 20° . Figure 5(b) shows the magnified (110) cross-sectional image corresponding to Figure 9(a). It is well understood that the apparently irregular cross-sectional growth pattern reflecting the rough surface is really composed of the $(\bar{1}\bar{1}1)B$ (the generation points are indicated by arrows) and $(\bar{1}13)B$ facets.

3. [100] stripe

Figure 10 shows (110) cross-sectional views of the as-etched profiles of the sidewalls of the [100] stripes with various values of θ . The HF+H₂O₂+H₂O mixtures used produced round intersection profiles between the sidewall and the lower substrate plane for large θ . Since the [100] stripe does not intersect the (110) cleavage plane at right angles as shown in Figure 1, the actual value of θ was evaluated from the experimentally observed apparent value, θ' , on the SEM photographs using the equation $\theta = \tan^{-1}(\tan\theta'/\cos 45^\circ)$. Figure 11 shows (110) cross-sectional views of the corresponding grown layers. Generation of extra facets on the sidewalls is described as follows:

(a)-(c) For $\theta > 45^\circ$, extra (031) and (011) facets with $\theta_f = 72^\circ$ and 45° were clearly identified. As θ became closer to 45° , the (011) facet developed more towards the sidewall, while the (031) facet diminished and finally disappeared.

(d)-(f) For $45^\circ \geq \theta > 19^\circ$, the (011) facet disappeared and an extra (013) facet with $\theta_f = 19^\circ$ appeared. As θ approached 19° , the (013) facet also developed more to-

wards the sidewall. The generation of an extra (045) facet with $\theta_f=38^\circ$, as shown in (e), is interesting in that the facet exists on the sidewalls with $\theta < 38^\circ$, that is, θ_f of the facet, does not follow the general rule of facet generation behavior. We speculate that the (045) facet actually exists for $\theta=43^\circ$ (Figure 12(e) below), 39° , and 21° ((d) and (f) of this figure), that is, the (045) facet accompanies the (013) facet.

(g)-(h) For $\theta \leq 19^\circ$, the (013) facet (and the (045) facet) also disappeared and no other extra facets were observed.

Figure 12 shows bird's eye views of the growth behavior of the (011) facet with respect to θ . The surface of the (011) facet shows the characteristic features reported in the literature [33-36]. It is well understood again from (a)-(d) that the (011) facet developed more towards the sidewall as θ approached 45° . It should be noted from comparison between (d) and (e) that only a 4° difference in θ caused a significant difference in facet generation behavior.

Figure 13 shows bird's eye views of the growth behavior of the (013) facet with respect to θ . It is well understood from (a)-(d) that the (013) facet developed more towards the sidewall and the surface of the facet became wavy as θ approached 19° .

Table 1 summarizes the facet generation behavior for the [100] stripe. In order to maintain the initial as-etched profile of the sidewall after growth, it is necessary to keep θ smaller than 19° . It was, however, impossible to obtain a flatness and uniformity of the sidewall layers that was comparable to those for the $[\bar{1}10]$ stripes with $\theta \leq 21^\circ$ (compare Figure 13(e) with Figure 4(f)), probably due to the high-index nature of the sidewalls.

Recently, growth of the (011) facet on the [100] stripe with the (010) sidewall, and quantum wires formed taking advantage of the (011) facet growth have been reported [20]. In [20], it has been shown that the (011) and (013) facets coexist in growth under low temperatures and/or high As_4 pressures. This will be discussed in connection with the orientation-dependent Ga surface diffusion length in Paper III.

4. Intersections of orthogonal stripes

In Paper I, the growth behavior on the corners of ridge-type triangles on the (111)A substrates, in other words, on the intersection of two crystallographically equivalent sidewalls, was investigated. Since the (001) surface has two-fold rotational symmetry (Figure 1), it will be interesting to study the growth behavior on the intersection of the nonequivalent $[\bar{1}10]$ and $[110]$ stripes and on the two nonequivalent intersections of the equivalent $[100]$ and $[010]$ stripes, that is, the “(111)A-related corner” and “ $(\bar{1}\bar{1}1)$ B-related corner”. The first systematic study of the growth behaviors on these intersections is presented below.

(1) Intersection of $[\bar{1}10]$ and $[110]$ stripes

Figure 14 shows top views of the as-etched profiles of the intersections of the $[\bar{1}10]$ and $[110]$ stripes with various values of θ . Figure 15 shows top views of the corresponding intersections after growth. Generation of extra facets on the corners was observed. Although they could not be definitely identified due to the non-flat and different as-etched profiles of the orthogonal sidewalls and to the occurrence of complicated sidewall profiles at the intersection, the following assignments will be reasonable from the discussion in the previous section:

- (a)-(d) For these intersections, the extra facet that appeared seems to be (011).
- (e)-(g) For these intersections, the extra facet that appeared seems to be (013).
- (h)-(j) For these intersections, no extra facets are observed.

The growth behaviors on the $[\bar{1}10]$ and $[110]$ stripes can be more distinctly compared in Figure 15. The surface morphology is better for the layers on the (111)A-related sidewalls than for those on the $(\bar{1}\bar{1}1)$ B-related sidewalls. This may be attributed, first, to the present growth conditions optimized for the (111)A surface and, second, to the anisotropic structure of the (2×4) -reconstructed (001) surface [37] during MBE. The latter has been demonstrated by a distinct difference in the straightness of microsteps produced by misorientations towards the $[\bar{1}10]$ and $[110]$ directions using scanning tunneling microscopy [38, 39]. It should, however, be noted from (h) that flat and uniform layers can be simultaneously grown on both types of sidewalls for θ around 20° only, that is, on the (111)A and

$(\bar{1}14)$ B sidewalls. This suggests that the $(\bar{1}\bar{1}3)$ B and $(\bar{1}\bar{1}4)$ B surfaces may have wider optimum growth conditions, which are closer to the optimum growth conditions for the (001) surface, than the $(\bar{1}\bar{1}\bar{1})$ B surface does.

(2) Intersections of [100] and [010] stripes

Figure 16 shows top views of the as-etched profiles of the intersections of the [100] and [010] stripes with various values of θ . There is no difference observed between the as-etched (111)A-related and $(\bar{1}\bar{1}\bar{1})$ B-related corners. Figure 17 shows top views of the corresponding intersections after growth. The following points can be well observed: Poor morphologies of the sidewall layers compared to those for the [110] stripes, the equivalency of the growth behaviors on the [100] and [010] stripes and, to be in sharp contrast to this, the nonequivalency of the growth behaviors on the (111)A-related and $(\bar{1}\bar{1}\bar{1})$ B-related corners. Especially in (f)-(h), extra facets are generated on the (111)A-related corners but not on the $(\bar{1}\bar{1}\bar{1})$ B-related corners. The identification of these facets was made on the basis of their orientations and of the values of θ_f evaluated as follows: The angle θ_c of the intersection line to the (001) substrate plane can be evaluated from the experimentally determined value of θ using the simple relation $\theta_c = \tan^{-1}(\tan\theta/\sqrt{2})$. The value of $\theta = 19^\circ$, estimated as corresponding to the onset boundary of the facets, gives the value of $\theta_c = 13^\circ$. This value corresponds to θ_f of the (116)A plane. The (111)A-related facets presented in Figures 17(g) and (h) correspond to (119)A and (1113)A, respectively. Table 1 also summarizes the facet generation behavior at the intersections of the [100] and [010] stripes. This result implies that it is impossible to grow GaAs and AlGaAs layers by MBE on ridge-type squares formed by the [100] and [010] stripes without modifying the initial as-etched pattern.

5. Phenomena common to three stripe patterns

Although the three stripes showed their respective facet generation behaviors as discussed above, the following point is worth mentioning as common to the three stripes: The persistent facets generating on the three stripes, that is, the (114)A facet on the $[\bar{1}10]$ stripe, the $(\bar{1}\bar{1}3)$ B facet on the [110] stripe, and the

(013) facet on the [100] stripe, have θ_f in the narrow range of 19° to 24° . This point seems to be related to the crystal structure of GaAs composed of the tetrahedral Ga-As bonding, as was also suggested for the (111)A patterned substrate in Paper I.

6. Comparison with (111)A patterned substrates

Comparing the facet generation behavior during MBE between the (001) patterned substrate described in the present paper and the (111)A patterned substrate described in Paper I, the following common and different features are pointed out:

(1) Growth of extra (114)A, (110), and $(\bar{1}\bar{1}\bar{1})$ B facets are common to the (111)A and (001) patterned substrates. Growth of extra (001), (113)A, (159), $(\bar{2}38)$, and $(\bar{1}25)$ facets are specific to the (111)A patterned substrates and growth of extra (111)A, $(\bar{1}13)$ B, (031), (045), and (013) facets are specific to the (001) patterned substrates.

(2) The general facet generation rule, that a facet present for large θ laterally develops more towards the sidewall as θ approaches θ_f of the facet and vanishes once θ decreases below θ_f , holds for both substrates. Although there are some facets that do not follow the rule, this does not result from the substrate orientation but from the special properties of the facets themselves.

(3) There is a critical value for θ below which flat and uniform layers on the sidewall and substrate plane grow maintaining the initial as-etched profile with no extra facets. The value is located in the narrow range of 33° to 35° independent of the sidewall orientation for the (111)A substrates, whereas it varies between 10° and 24° depending on the sidewall orientation for the (001) substrates.

(4) The steps with $\theta_f=16^\circ-17^\circ$ appear near the sidewall-substrate plane boundary independent of the sidewall orientation for the (111)A substrates while no steps are observed for the (001) substrates.

These points reflect not only differences in the crystallographic, chemical, and thermodynamic properties between the two substrates but also differences in the

interaction of adatoms between the substrate plane and adjacent sidewall. These points will be discussed in more detail in Paper III.

4. Summary and Conclusion

Extra facet generation during MBE growth of GaAs/AlGaAs multilayers on (001) GaAs substrates patterned with stripes running in the $[\bar{1}10]$, $[110]$, and $[100]$ directions and having various slopes, designated as " $[\bar{1}10]$ stripe", " $[110]$ stripe", and " $[100]$ stripe", respectively, has systematically been investigated for the first time. It has been confirmed that extra (111)A and (114)A facets generated on the $[\bar{1}10]$ stripes, extra $(\bar{1}11)$ B and $(\bar{1}13)$ B facets on the $[110]$ stripes, and extra (031), (011), (045), and (013) facets on the $[100]$ stripes, depending on the intersection angle θ of the side wall and the substrate plane. Among them, the (114)A, $(\bar{1}13)$ B, and (013) facets are important because they persist for a wide range of θ and, therefore, play a detrimental role in forming flat and uniform sidewall layers on the (001) patterned substrates. It has been made clear that no extra facets generate on the sidewalls and flat and uniform layers maintaining the initial as-etched stripe patterns can be grown for the $[\bar{1}10]$ stripes with $10^\circ \geq \theta$, the $[110]$ stripes with $24^\circ \geq \theta \geq 20^\circ$, and the $[100]$ stripes with $19^\circ \geq \theta$. Extra (111)A-related facets have developed on the (111)A-related intersection of the equivalent $[100]$ and $[010]$ stripes, while no extra facets have developed on the $(\bar{1}11)$ B-related intersection. The (114)A, $(\bar{1}\bar{1}\bar{1})$ B, and (110) facets have been confirmed as common to the (111)A and (001) patterned substrates.

-ACKNOWLEDGMENTS-

The authors would like to thank Dr. Y. Furuhashi for his encouragement throughout this work.

-REFERENCES-

- [1] W. T. Tsang and A. Y. Cho, *Appl. Phys. Lett.* **30**, 293 (1977).
- [2] J. S. Smith, P. L. Derry, S. Margalit, and A. Yariv, *Appl. Phys. Lett.* **47**, 712 (1985).
- [3] D. L. Miller, *Appl. Phys. Lett.* **47**, 1309 (1985).
- [4] T. Yuasa, M. Manno, T. Yamada, S. Narituka, K. Shinozaki, and M. Ishii, *J. Appl. Phys.* **62**, 764 (1987).
- [5] E. Kapon, M. C. Tamargo, and D. M. Hwang, *Appl. Phys. Lett.* **50**, 347 (1987).
- [6] H. P. Meier, R. F. Broom, P. W. Epperlein, E. van Gieson, Ch. Harder, H. Jäckel, W. Walter, and D. J. Webb, *J. Vac. Sci. Technol. B* **6**, 692 (1987).
- [7] H. P. Meier, E. van Gieson, R. F. Broom, W. Walter, D. J. Webb, C. Harder, and H. Jäckel, *Inst. Phys. Conf. Ser. No.91*, 609 (1988).
- [8] S. Nilsson, E. van Gieson, D. J. Arent, H. P. Meier, W. Walter, and T. Forster, *Appl. Phys. Lett.* **55**, 972 (1989).
- [9] D. J. Arent, S. Nilsson, Y. D. Galeuchet, H. P. Meier, and W. Walter, *Appl. Phys. Lett.* **55**, 2611 (1989).
- [10] M. Hata, T. Isu, A. Watanabe, and Y. Katayama, *Appl. Phys. Lett.* **56**, 2542 (1990).
- [11] M. Hata, T. Isu, A. Watanabe, and Y. Katayama, *J. Vac. Sci. Technol. B* **8**, 692 (1990).
- [12] Y. Nakamura, S. Koshihara, M. Tsuchiya, H. Kano, and H. Sakaki, *Appl. Phys. Lett.* **59**, 700 (1991).
- [13] X. Q. Shen, M. Tanaka, and T. Nishinaga, *10th Symp. Rec. Alloy Semicond. Phys. Electron.* **65** (1991).
- [14] S. Shimomura, S. Ohkubo, Y. Yuba, S. Namba, S. Hiyamizu, M. Shigeta, T. Yamamoto, and K. Kobayashi, *Surf. Sci.* **267**, 13 (1992).
- [15] Y. Morishita, Y. Momura, S. Goto, Y. Katayama, and T. Isu, *Inst. Phys. Conf. Ser. No.120*, 19 (1992).

- [16] X. Q. Shen, M. Tanaka, and T. Nishinaga, 11th Symp. Rec. Alloy Semicond. Phys. Electron. 333 (1992).
- [17] X. Q. Shen and T. Nishinaga, 12th Symp. Rec. Alloy Semicond. Phys. Electron. 367 (1993).
- [18] M. Walther, T. Röhr, G. Böhm, G. Tränkle, and G. Weimann, J. Crystal Growth 127, 1045 (1993).
- [19] H. Saito, M. Sugimoto, M. Anan, Y. Ochiai, Jpn. J. Appl. Phys. 32, L1034 (1993).
- [20] M. López, T. Ishikawa, and Y. Nomura, Jpn. J. Appl. Phys. 32, L1051 (1993).
- [21] X. Q. Shen and T. Nishinaga, Jpn. J. Appl. Phys. 32, L1117 (1993).
- [22] T. Takebe, T. Yamamoto, M. Fujii, and K. Kobayashi, J. Electrochem. Soc. 140, 1169 (1993).
- [23] T. Yamamoto, M. Inai, T. Takebe, M. Fujii, and K. Kobayashi, J. Crystal Growth 127, 865 (1993).
- [24] K. Tsutsui, H. Mizukami, O. Ishiyama, S. Nakamura, and S. Furukawa, Jpn. J. Appl. Phys. 29, 468 (1990).
- [25] P. Chen, K. C. Rajkumar, and A. Madhukar, Appl. Phys. Lett. 58, 1771 (1991).
- [26] T. Hayakawa, M. Nagai, M. Morishima, H. Horie, and K. Matsumoto, Appl. Phys. Lett. 59, 2287 (1991).
- [27] T. Hayakawa, M. Morishima, and S. Chen, Appl. Phys. Lett. 59, 3321 (1991).
- [28] T. Hayakawa, M. Morishima, M. Nagai, H. Horie, and K. Matsumoto, Surf. Sci. 267, 8 (1992).
- [29] J. Fu, K. Zhang, and D. L. Miller, J. Vac. Sci. Technol. B 10, 779 (1992).
- [30] D. A. Woolf, Z. Sobiesierski, D. I. Westwood, and R. H. Williams, J. Appl. Phys. 71, 4908 (1992).
- [31] D. A. Woolf, J. P. Williams, D. I. Westwood, Z. Sobiesierski, J. E. Aubrey, and R. H. Williams, J. Crystal Growth 127, 913 (1993).

- [32] T. Isu, Y. Morishita, S. Goto, Y. Nomura, and Y. Katayama, *J. Crystal Growth* **127**, 942 (1993).
- [33] J. M. Ballingall and C. E. C. Wood, *Appl. Phys. Lett.* **41**, 947 (1982).
- [34] W. I. Wang, *J. Vac. Sci. Technol. B* **1**, 630 (1983).
- [35] L. T. Parechian, E. R. Weber, T. L. Hierl, *Mat. Res. Soc. Symp. Proc.* **46**, 391 (1985).
- [36] L. T. P. Allen, E. R. Weber, J. Washburn, Y. C. Pao, and A. G. Elliot, *J. Crystal Growth* **87**, 193 (1988).
- [37] M. D. Pashley, K. W. Habarern, W. Friday, J. M. Woodall, and P. D. Kirchner, *Phys. Rev. Lett.* **60**, 2176 (1988).
- [38] M. D. Pashley, K. W. Habarern, J. M. Gaines, *Appl. Phys. Lett.* **58**, 406 (1991).
- [39] M. D. Pashley, K. W. Habarern, J. M. Gaines, *Surf. Sci.* **267**, 153 (1992).

-FIGURE CAPTIONS-

Figure 1 Schematic presentation of $[\bar{1}10]$, $[110]$, $[100]$, and $[010]$ stripes formed on the GaAs (001) surface.

Figure 2 $(\bar{1}10)$ cross-sectional views of the as-etched profiles of the (111)A-related sidewalls of the $[\bar{1}10]$ stripes with various slopes.

Figure 3 $(\bar{1}10)$ cross-sectional views of the after-growth profiles of the (111)A-related sidewalls corresponding to Figure 2.

Figure 4 Bird's eye views of the growth behavior of the (114)A facet (indicated by arrow) with respect to θ .

Figures 5 (a) Magnified $(\bar{1}10)$ cross-sectional view of the (111)A-related sidewall corresponding to Figure 4(b) and (b) Magnified (110) cross-sectional view of the $(\bar{1}11)$ B-related sidewall corresponding to Figure 9(a).

Figure 6 (110) cross-sectional views of the as-etched profiles of the $(\bar{1}11)$ B-related sidewalls of the $[110]$ stripes with various slopes.

Figure 7 (110) cross-sectional views of the after-growth profiles of the $(\bar{1}11)$ B-related sidewalls corresponding to Figure 6.

Figures 8 Bird's eye views of the growth behavior of the $(\bar{1}11)$ B facet (indicated by arrow) with respect to θ .

Figures 9 Bird's eye views of the growth behavior of the $(\bar{1}13)$ B facet (indicated by arrow) with respect to θ .

Figure 10 (110) cross-sectional views of the as-etched profiles of the (010)-related sidewalls of the $[100]$ stripes with various slopes.

Figure 11 (110) cross-sectional views of the after-growth profiles of the (010)-related sidewalls corresponding to Figure 10.

Figures 12 Bird's eye views of the growth behavior of the (011) facet (indicated by arrow) with respect to θ .

Figures 13 Bird's eye views of the growth behavior of the (013) facet (indicated by arrow) with respect to θ .

Figure 14 Top views of the as-etched profiles of the intersections of the $[\bar{1}10]$ and $[110]$ stripes with various sidewall slopes.

Figure 15 Top views of the after-growth profiles of the intersections of the $[\bar{1}10]$ and $[110]$ stripes corresponding to Figure 14.

Figure 16 Top views of the as-etched profiles of the intersections of the $[100]$ and $[010]$ stripes with various sidewall slopes.

Figure 17 Top views of the after-growth profiles of the intersections of the $[100]$ and $[010]$ stripes corresponding to Figure 16.

-TABLE HEADINGS-

Table 1 Summary of facet generation behavior during MBE on GaAs (001) patterned substrates.

STRIPES ON GaAs (001) SUBSTRATES

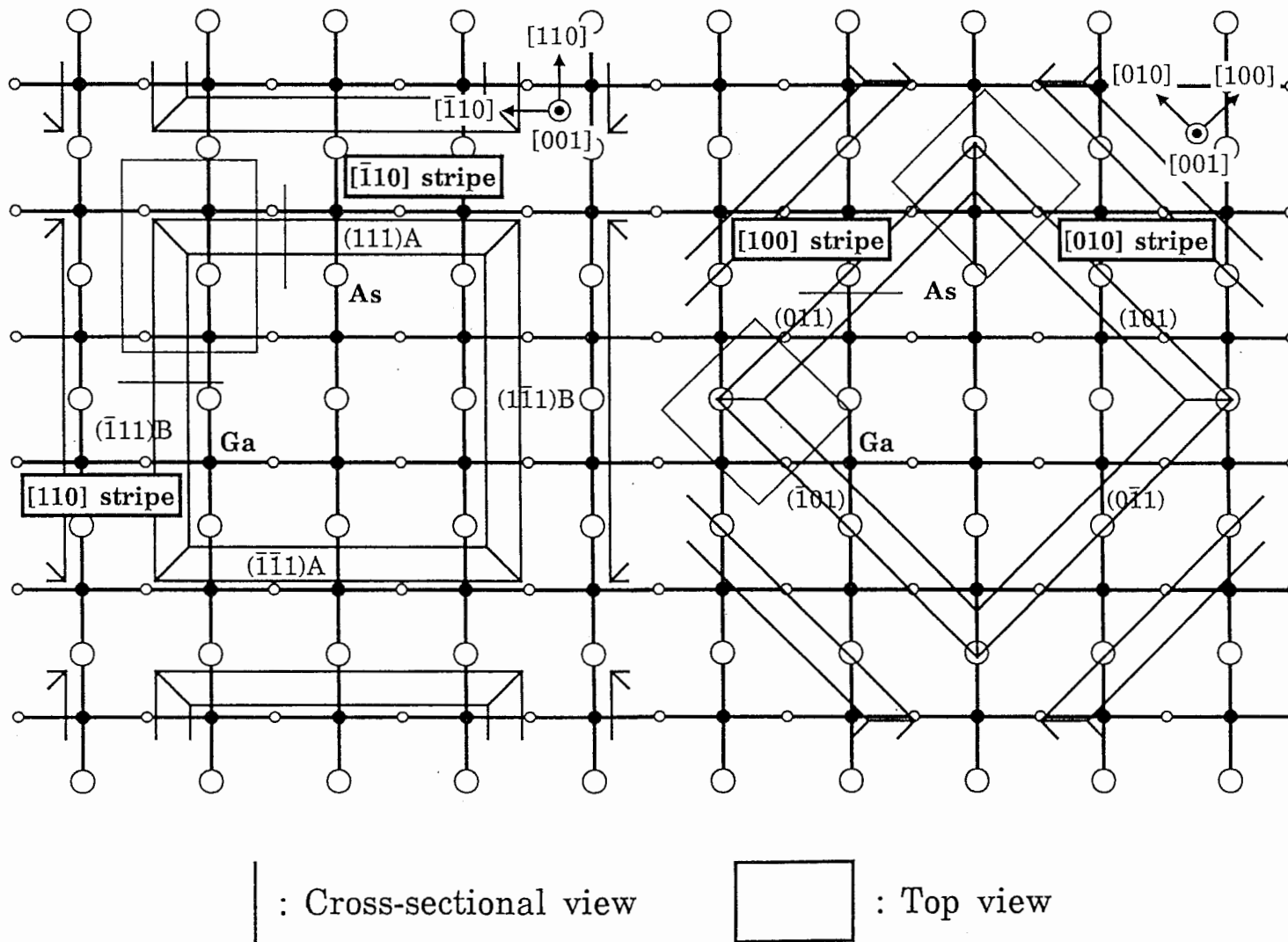
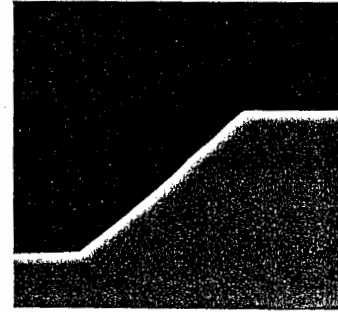
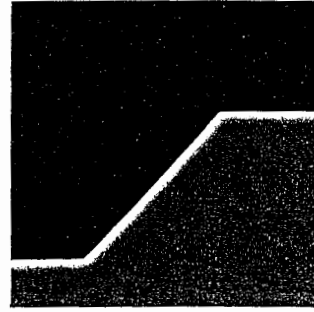
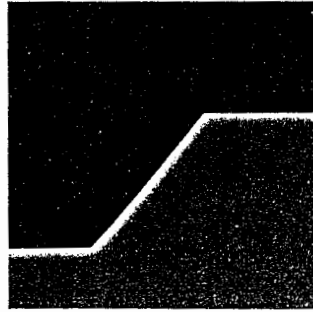
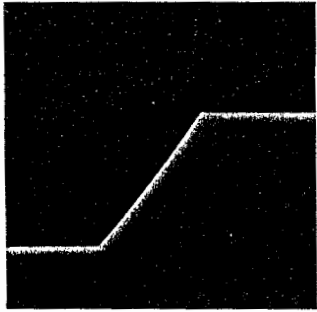


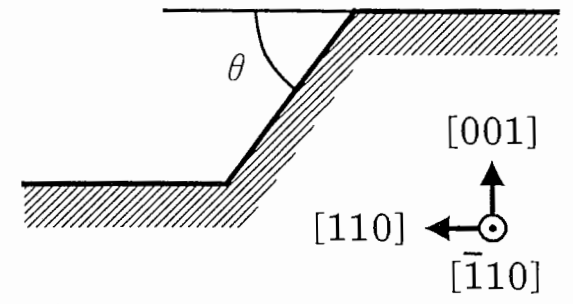
Figure 1 Schematic presentation of $[\bar{1}10]$, $[110]$, $[100]$, and $[010]$ stripes formed on the GaAs (001) surface.

HF : H₂O₂ : H₂O = x : y : z at 25 °C
 x = 0.05 mol / y = 0.04 - 0.34 mol / z = 1.22 - 56.82 mol

(a) $\theta = 54^\circ / (111)A$ (b) $\theta = 51^\circ / (889)A$ (c) $\theta = 48^\circ / (445)A$ (d) $\theta = 41^\circ / (335)A$



($\bar{1}10$) cross-sectional view

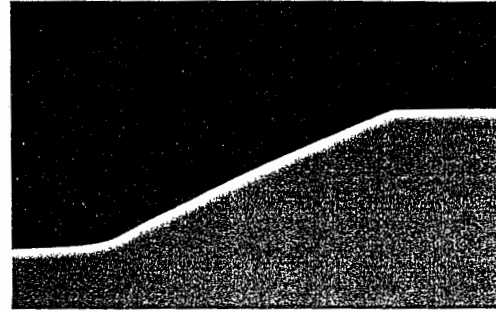
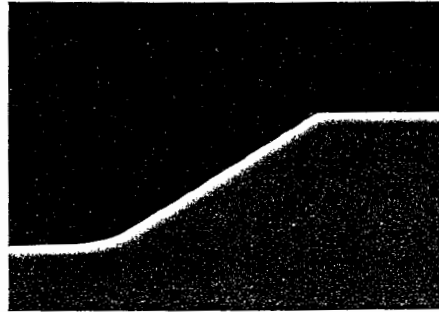
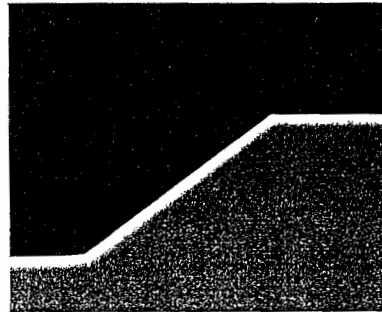


← GaAs substrate

(e) $\theta = 37^\circ / (112)A$

(f) $\theta = 32^\circ / (449)A$

(g) $\theta = 24^\circ / (113)A$



1 μm

(h) $\theta = 13^\circ / (116)A$

(i) $\theta = 9^\circ / (119)A$

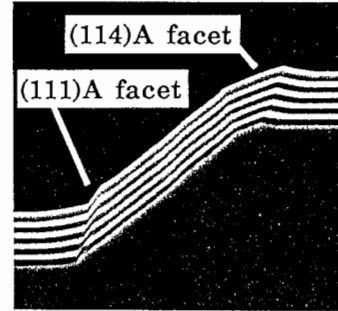
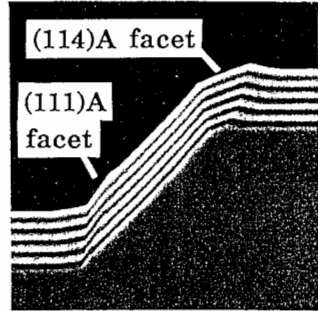
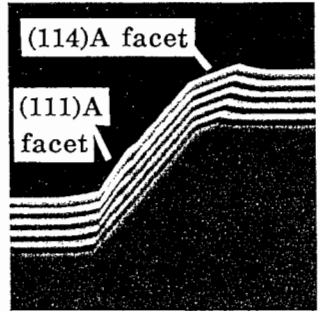
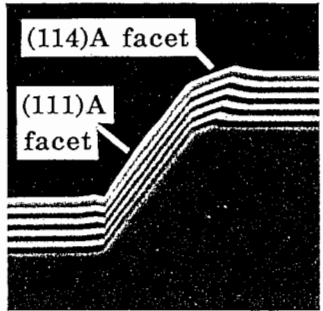


Figure 2 ($\bar{1}10$) cross-sectional views of the as-etched profiles of the (111)A-related sidewalls of the [$\bar{1}10$] stripes with various slopes.

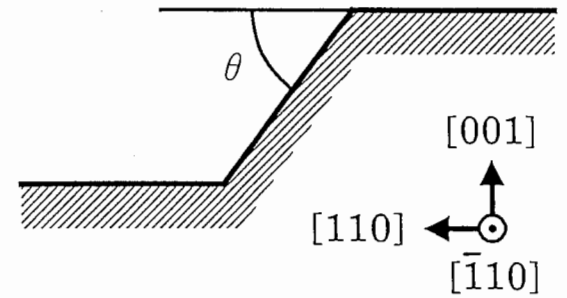
Growth temperature = 620 °C

V/III flux ratio = 7.4 (GaAs) / 6.2 (Al_{0.3}Ga_{0.7}As)

(a) $\theta = 54^\circ / (111)A$ (b) $\theta = 51^\circ / (889)A$ (c) $\theta = 48^\circ / (445)A$ (d) $\theta = 41^\circ / (335)A$



($\bar{1}10$) cross-sectional view

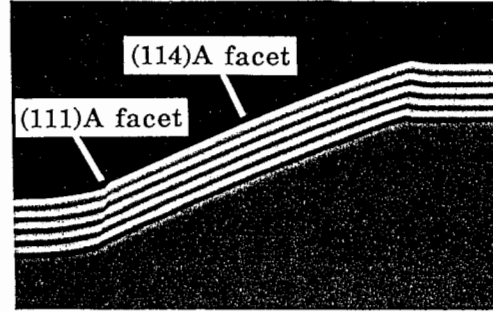
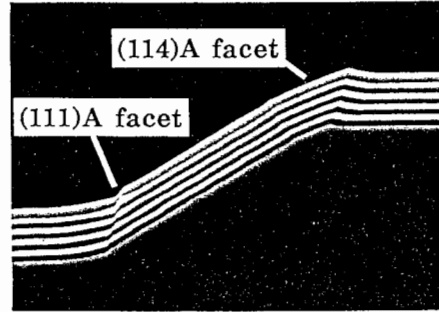
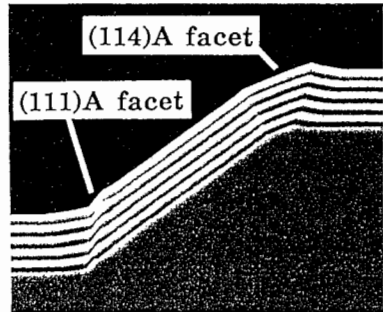


← GaAs substrate

(e) $\theta = 37^\circ / (112)A$

(f) $\theta = 32^\circ / (449)A$

(g) $\theta = 24^\circ / (113)A$



0.2 μm GaAs

0.2 μm Al_{0.3}Ga_{0.7}As

(h) $\theta = 13^\circ / (116)A$

(i) $\theta = 9^\circ / (119)A$

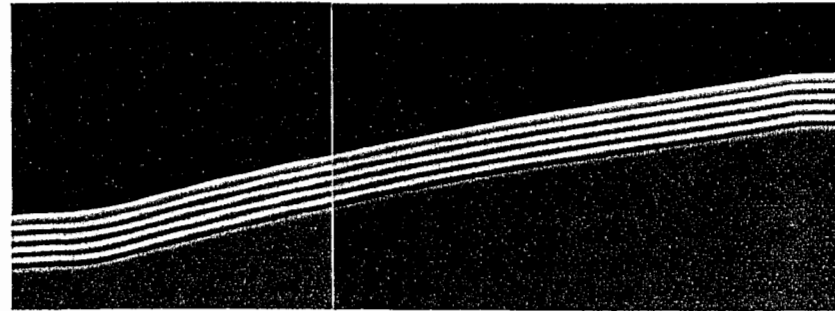
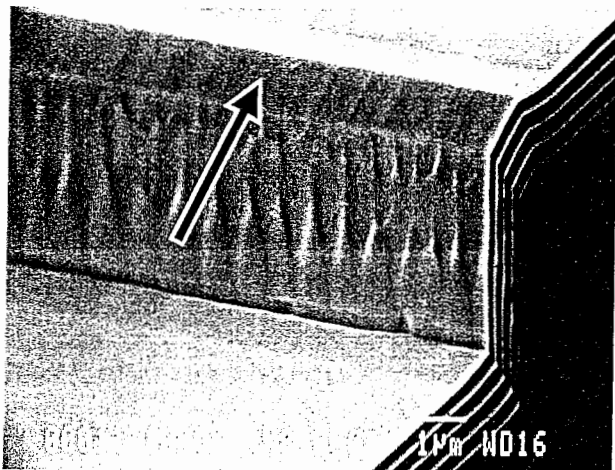


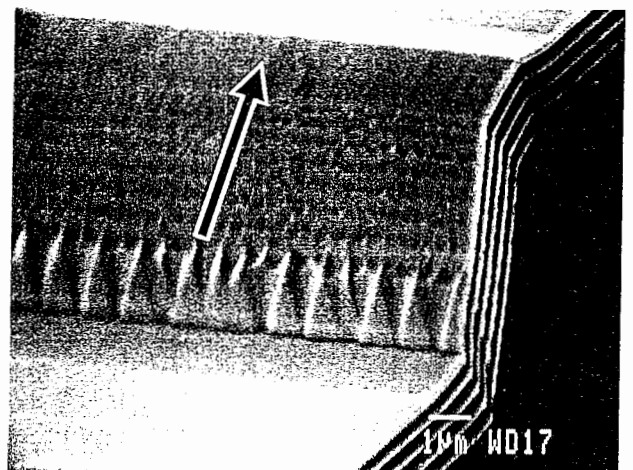
Figure 3 ($\bar{1}10$) cross-sectional views of the after-growth profiles of the (111)A-related sidewalls corresponding to Figure 2.

(114)A / $\theta_f = 21^\circ$

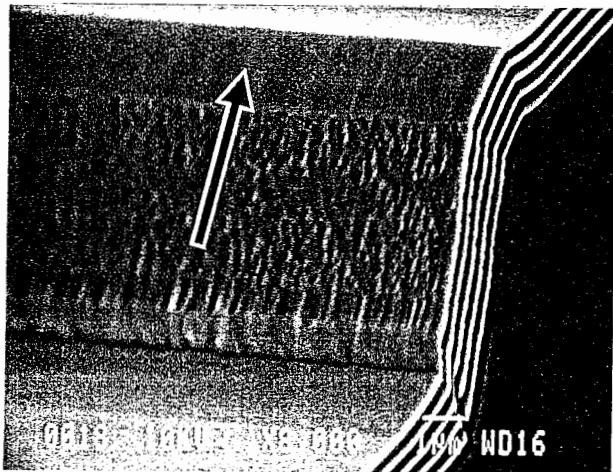
(a) $\theta = 54^\circ / (111)A$



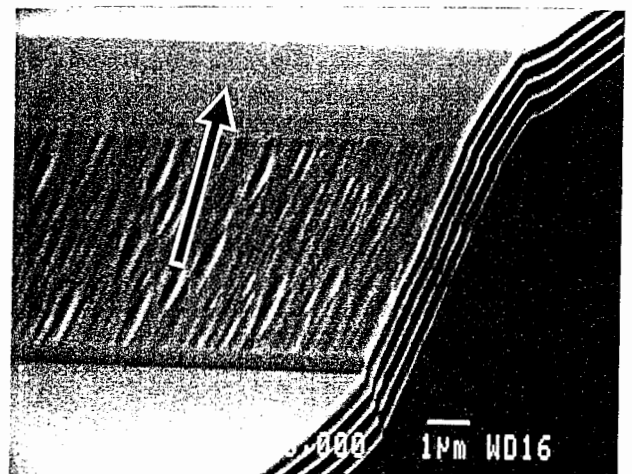
(b) $\theta = 48^\circ / (445)A$



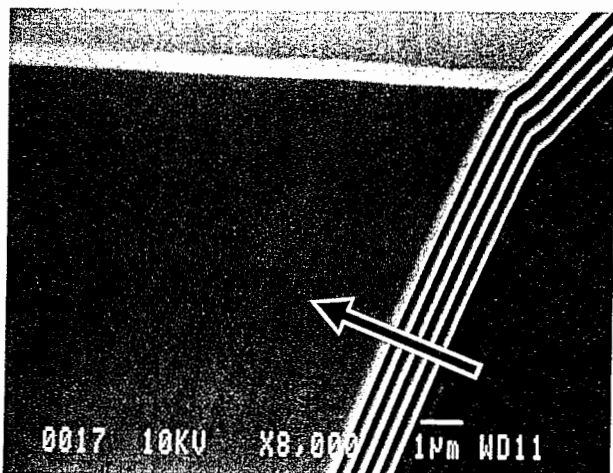
(c) $\theta = 41^\circ / (335)A$



(d) $\theta = 32^\circ / (449)A$



(e) $\theta = 24^\circ / (113)A$



(f) $\theta = 13^\circ / (116)A$

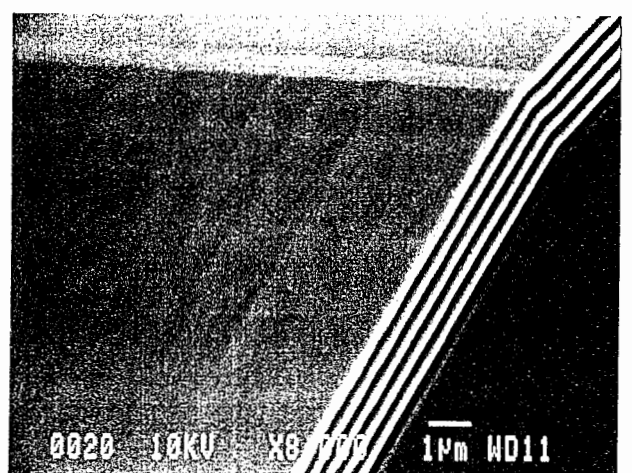
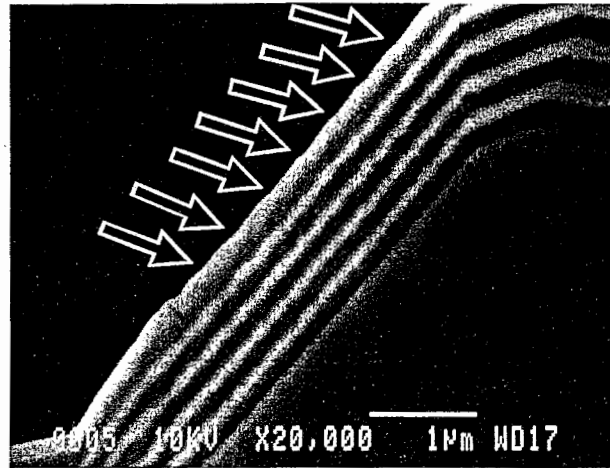


Figure 4 Bird's eye views of the growth behavior of the (114)A facet (indicated by arrow) with respect to θ .

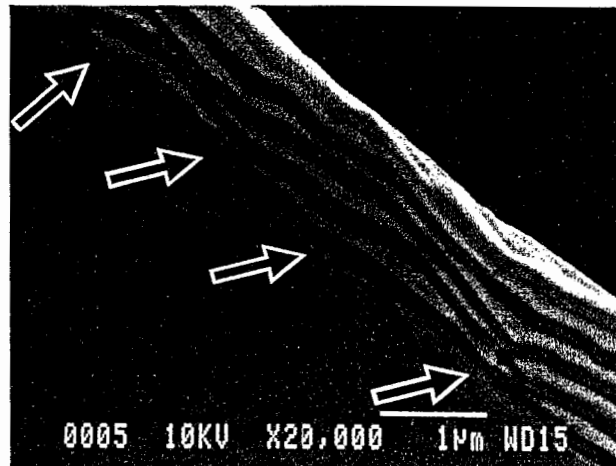
“ $[\bar{1}10]$ stripe”

(a) $\theta = 48^\circ / (445)A$



“ $[110]$ stripe”

(b) $\theta = 40^\circ / (\bar{3}35)B$



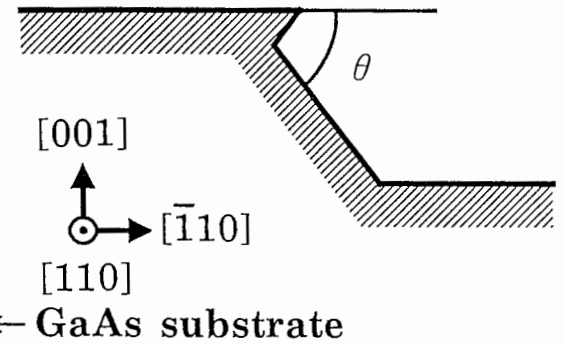
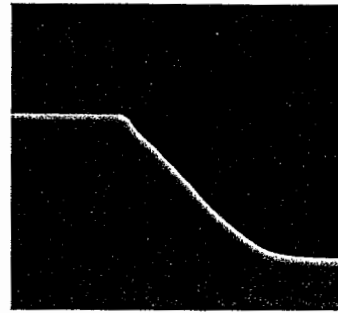
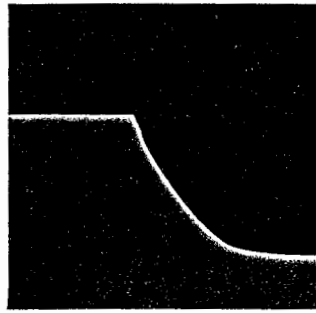
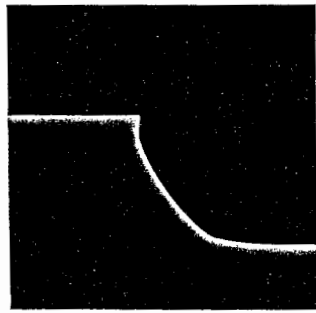
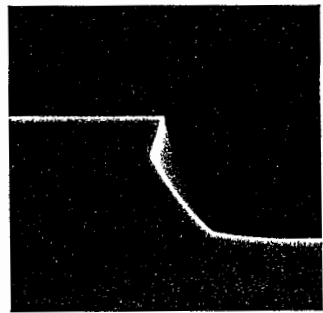
Figures 5 (a) Magnified $(\bar{1}10)$ cross-sectional view of the $(111)A$ -related sidewall corresponding to Figure 4(b) and (b) Magnified (110) cross-sectional view of the $(\bar{1}11)B$ -related sidewall corresponding to Figure 9(a).

HF : H₂O₂ : H₂O = x : y : z at 25 °C

x = 0.05 mol / y = 0.04 - 0.34 mol / z = 1.22 - 56.82 mol

(110) cross-sectional view

(a) $\theta = 57^\circ / (\bar{9}98)B$ (b) $\theta = 54^\circ / (\bar{1}11)B$ (c) $\theta = 52^\circ / (\bar{8}89)B$ (d) $\theta = 47^\circ / (\bar{3}34)B$

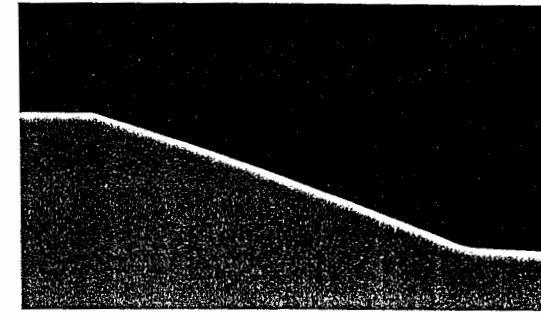
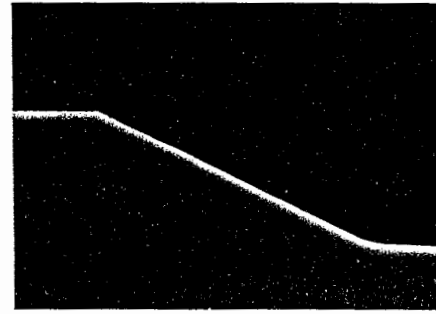
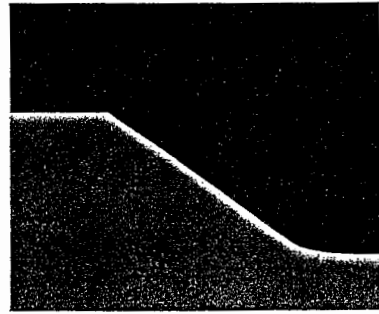
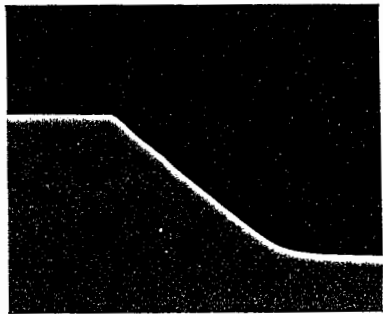


(e) $\theta = 40^\circ / (\bar{3}35)B$

(f) $\theta = 36^\circ / (\bar{1}12)B$

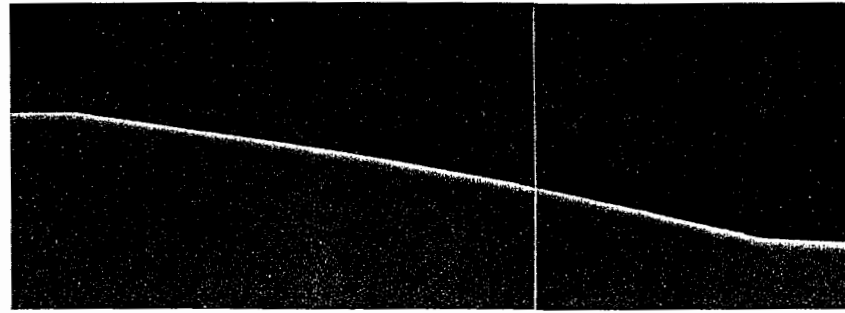
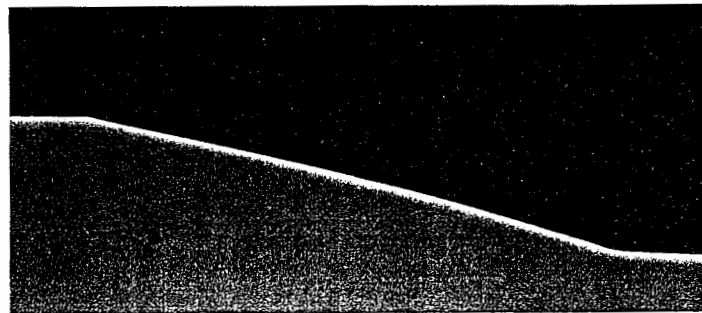
(g) $\theta = 26^\circ / (\bar{1}13)B$

(h) $\theta = 20^\circ / (\bar{1}14)B$



(i) $\theta = 12^\circ / (\bar{1}17)B$

(j) $\theta = 9^\circ / (\bar{1}19)B$



1 μm

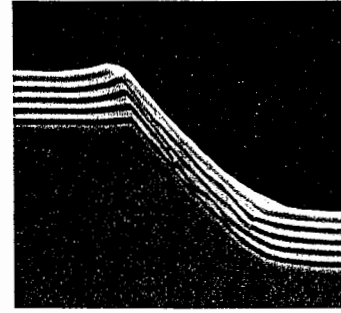
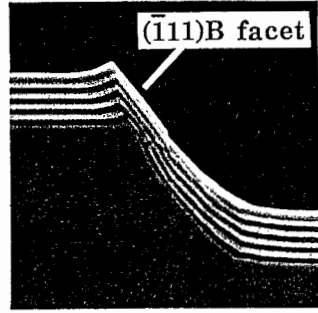
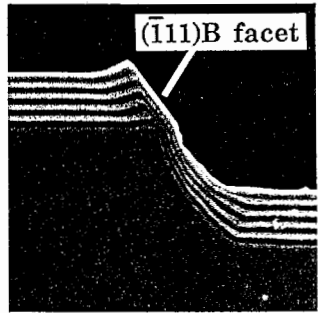
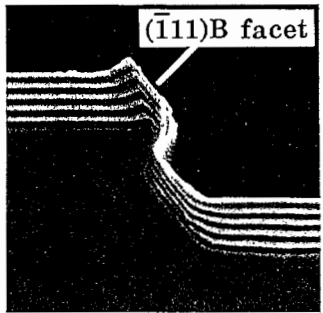
Figure 6 (110) cross-sectional views of the as-etched profiles of the $(\bar{1}11)B$ -related sidewalls of the [110] stripes with various slopes.

25

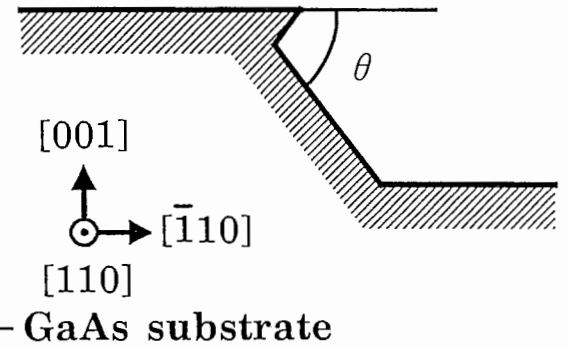
Growth temperature = 620 °C

V/III flux ratio = 7.4 (GaAs) / 6.2 (Al_{0.3}Ga_{0.7}As)

(a) $\theta = 57^\circ / (\bar{111})\text{B}$ (b) $\theta = 54^\circ / (\bar{111})\text{B}$ (c) $\theta = 52^\circ / (\bar{889})\text{B}$ (d) $\theta = 47^\circ / (\bar{334})\text{B}$



(110) cross-sectional view

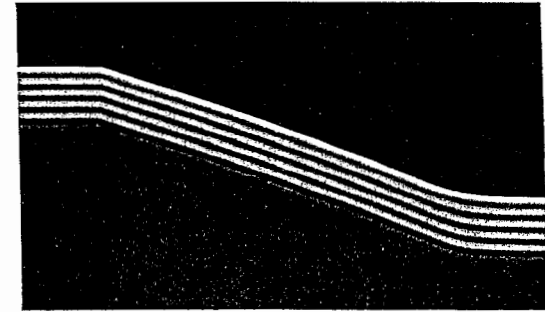
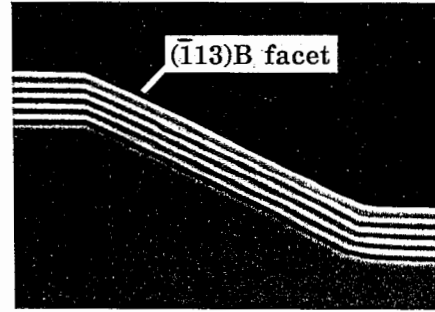
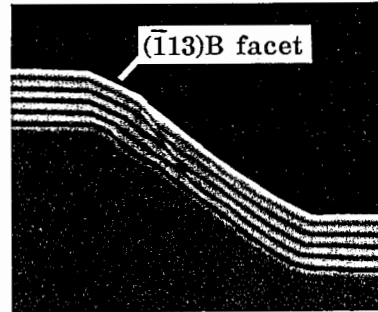
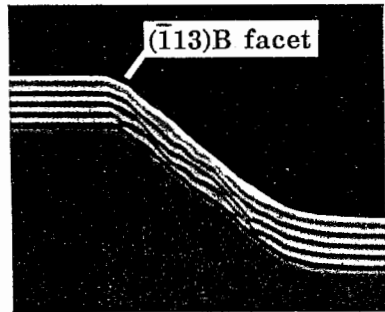


(e) $\theta = 40^\circ / (\bar{335})\text{B}$

(f) $\theta = 36^\circ / (\bar{112})\text{B}$

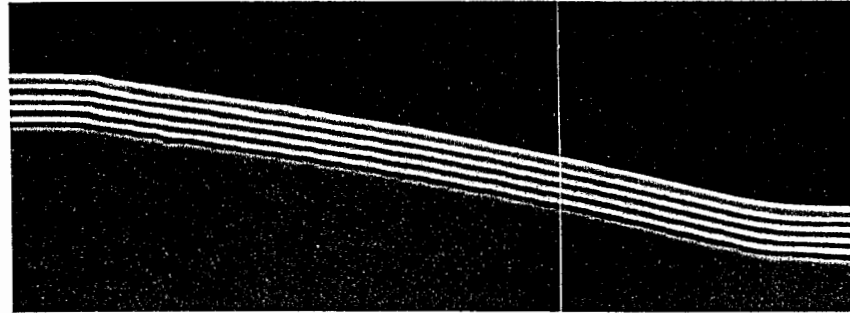
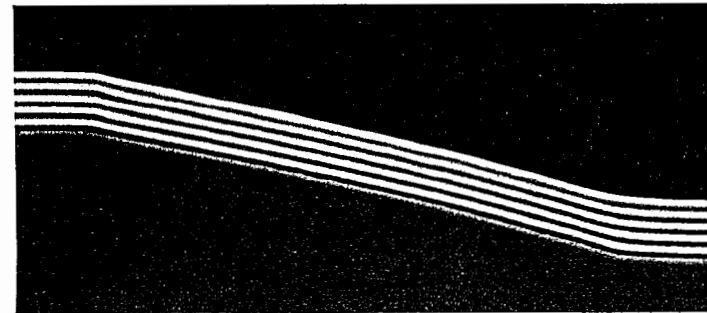
(g) $\theta = 26^\circ / (\bar{113})\text{B}$

(h) $\theta = 20^\circ / (\bar{114})\text{B}$



(i) $\theta = 12^\circ / (\bar{117})\text{B}$

(j) $\theta = 9^\circ / (\bar{119})\text{B}$



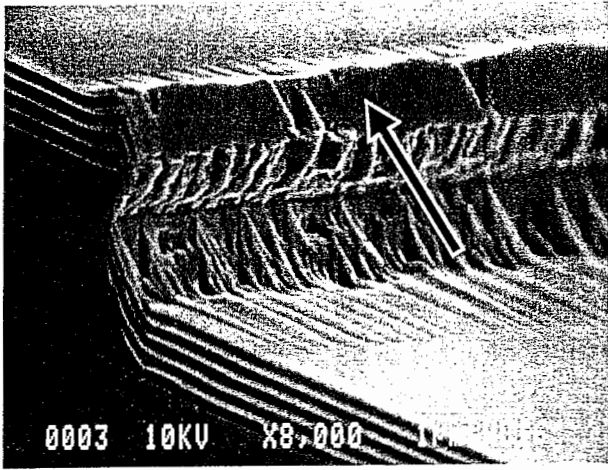
1 μm

0.2 μm GaAs
0.2 μm Al_{0.3}Ga_{0.7}As

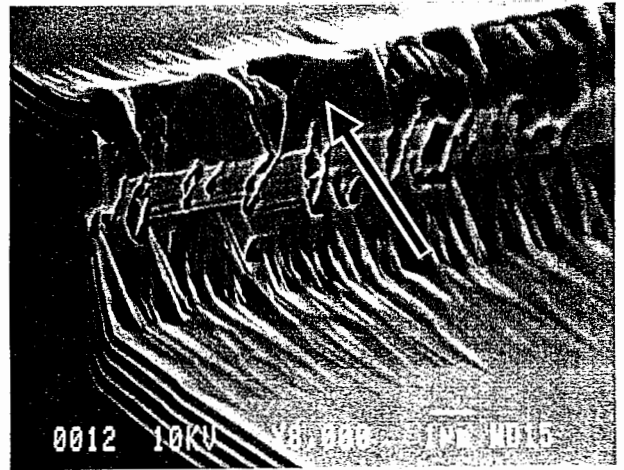
Figure 7 (110) cross-sectional views of the after-growth profiles of the $(\bar{111})\text{B}$ -related sidewalls corresponding to Figure 6.

$(\bar{1}11)B / \theta_f = 53^\circ$

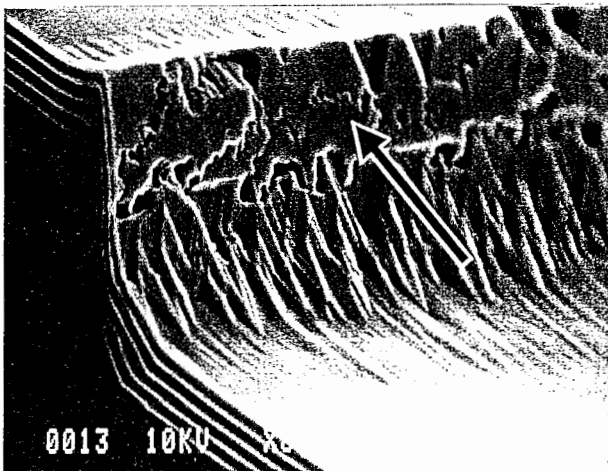
(a) $\theta = 57^\circ / (\bar{9}98)B$



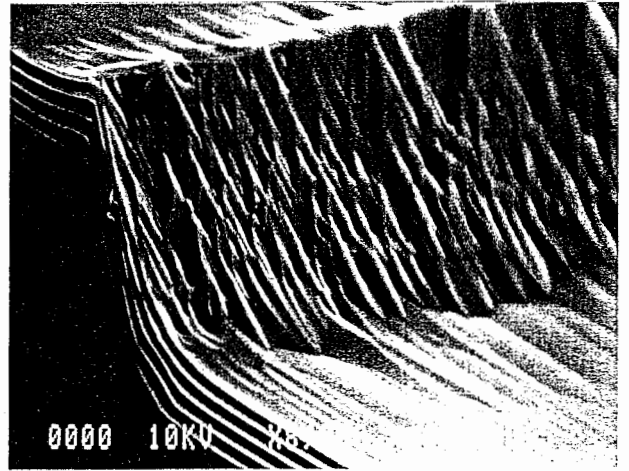
(b) $\theta = 54^\circ / (\bar{1}11)B$



(c) $\theta = 52^\circ / (\bar{8}89)B$



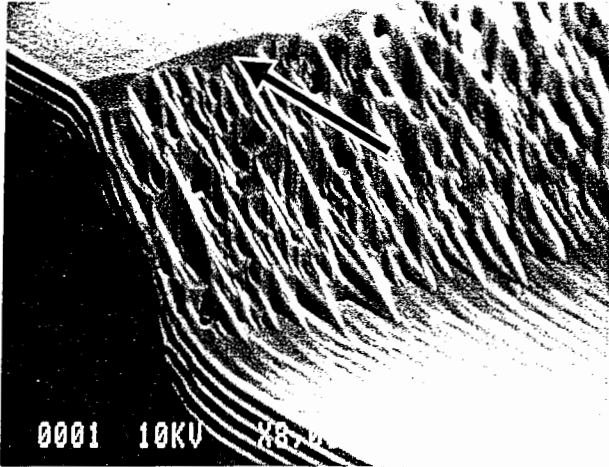
(d) $\theta = 47^\circ / (\bar{3}34)B$



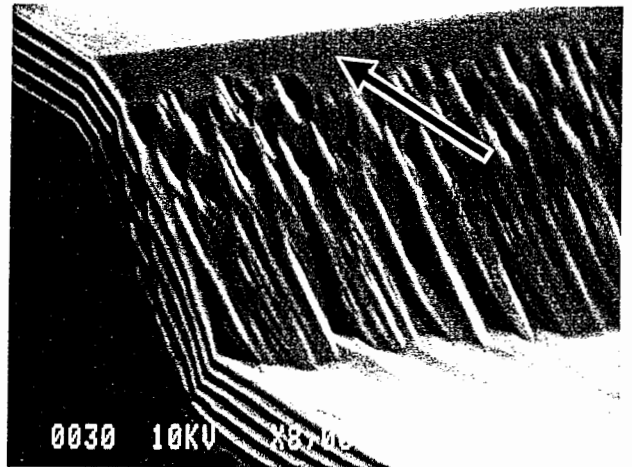
Figures 8 Bird's eye views of the growth behavior of the $(\bar{1}11)B$ facet (indicated by arrow) with respect to θ .

$(\bar{1}13)B / \theta_f = 24^\circ$

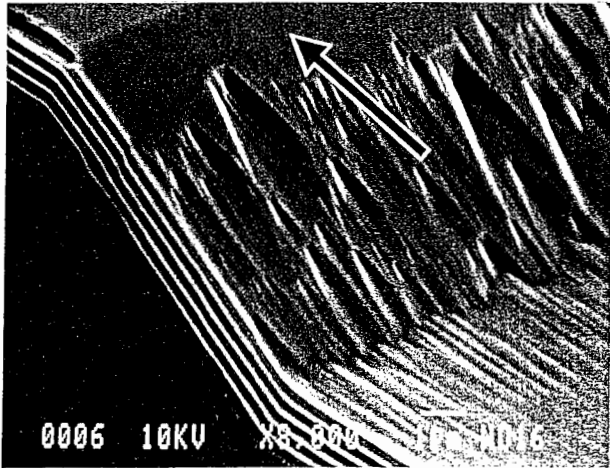
(a) $\theta = 40^\circ / (\bar{3}35)B$



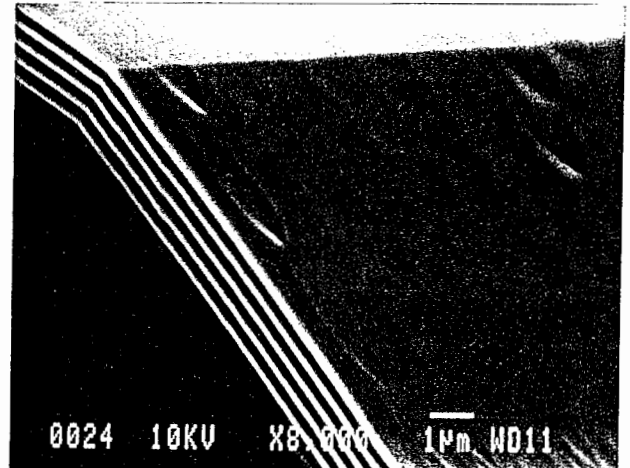
(b) $\theta = 36^\circ / (\bar{1}12)B$



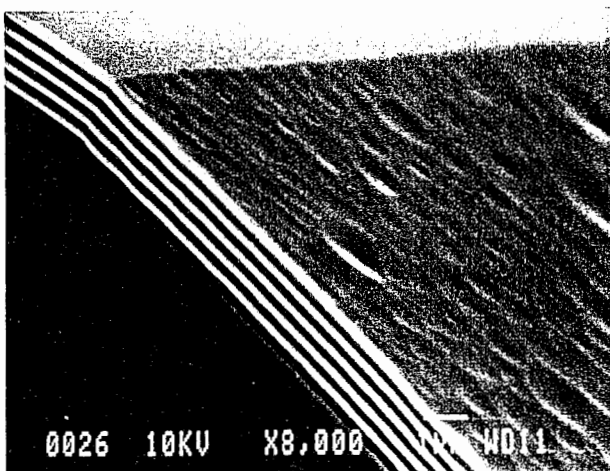
(c) $\theta = 26^\circ / (\bar{1}13)B$



(d) $\theta = 20^\circ / (\bar{1}14)B$



(e) $\theta = 12^\circ / (\bar{1}17)B$



Figures 9 Bird's eye views of the growth behavior of the $(\bar{1}13)B$ facet (indicated by arrow) with respect to θ .

HF : H₂O₂ : H₂O = x : y : z at 25 °C
 x = 0.05 mol / y = 0.04 - 0.34 mol / z = 1.22 - 56.82 mol

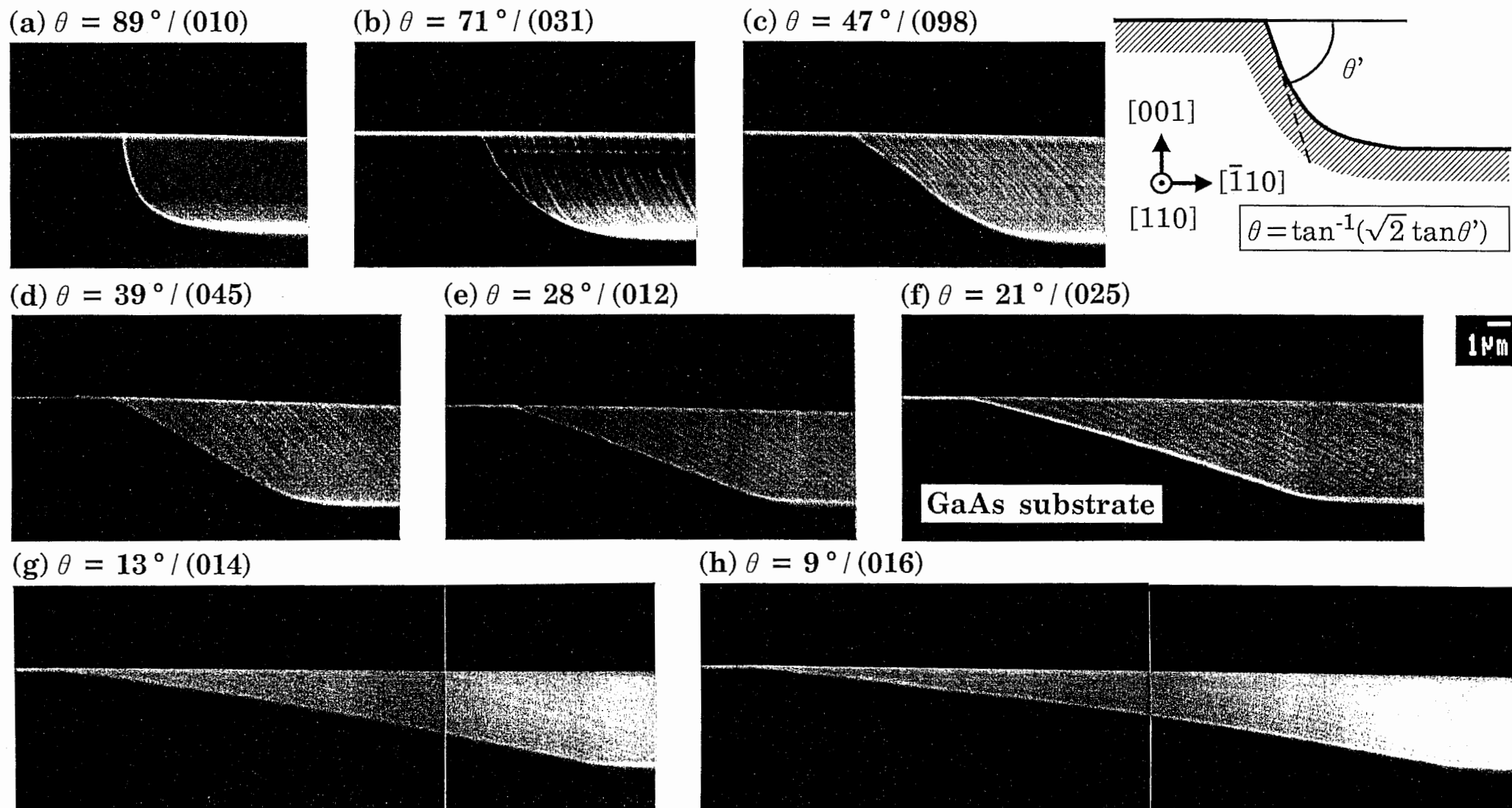
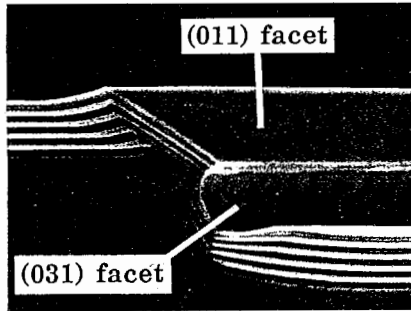


Figure 10 (110) cross-sectional views of the as-etched profiles of the (010)-related sidewalls of the [100] stripes with various slopes.

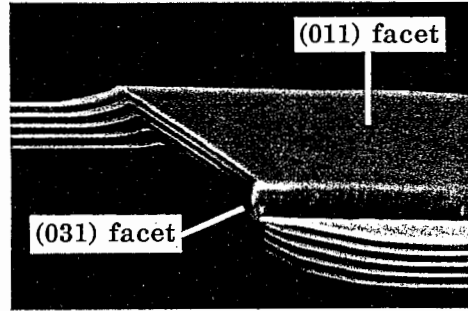
Growth temperature = 620 °C

V/III flux ratio = 7.4 (GaAs) / 6.2 (Al_{0.3}Ga_{0.7}As)

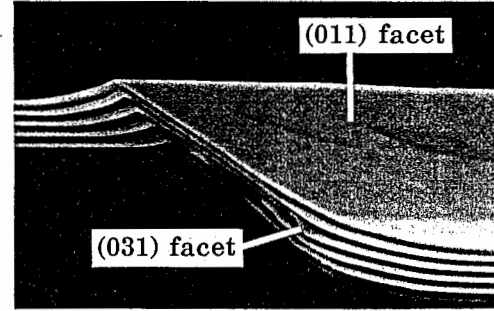
(a) $\theta = 89^\circ / (010)$



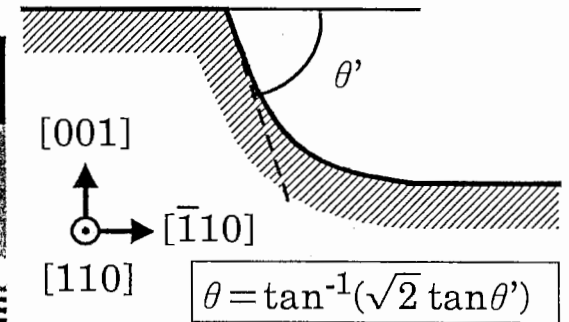
(b) $\theta = 71^\circ / (031)$



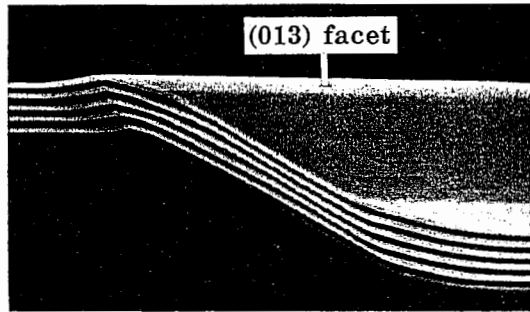
(c) $\theta = 47^\circ / (098)$



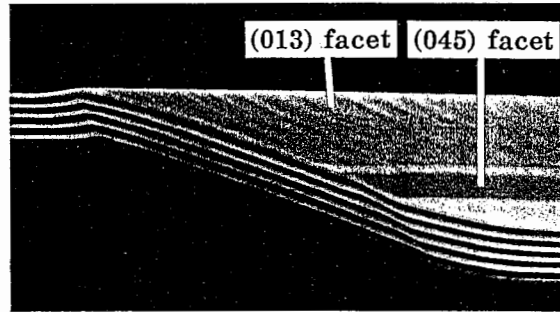
(110) cross-sectional view



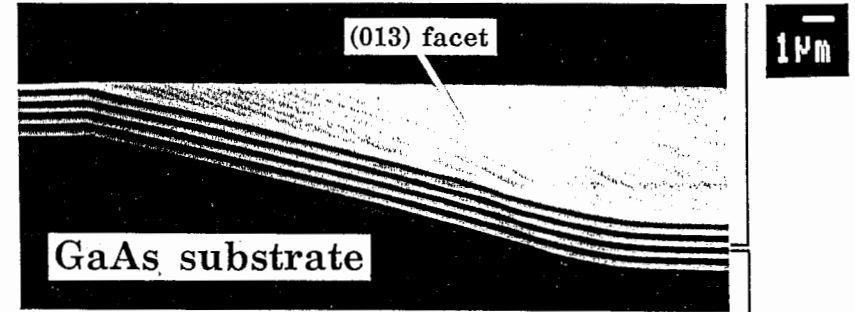
(d) $\theta = 39^\circ / (045)$



(e) $\theta = 28^\circ / (012)$



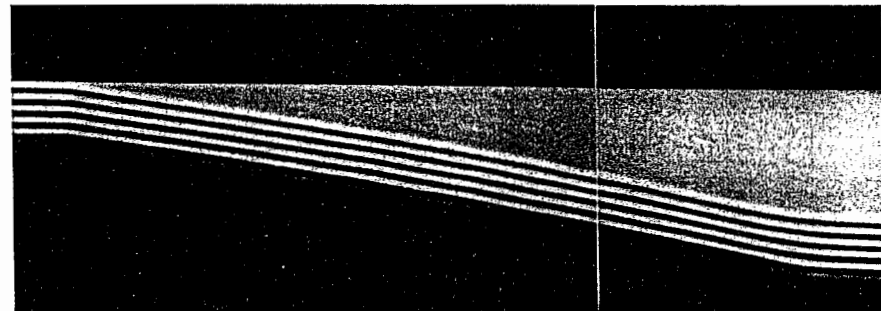
(f) $\theta = 21^\circ / (025)$



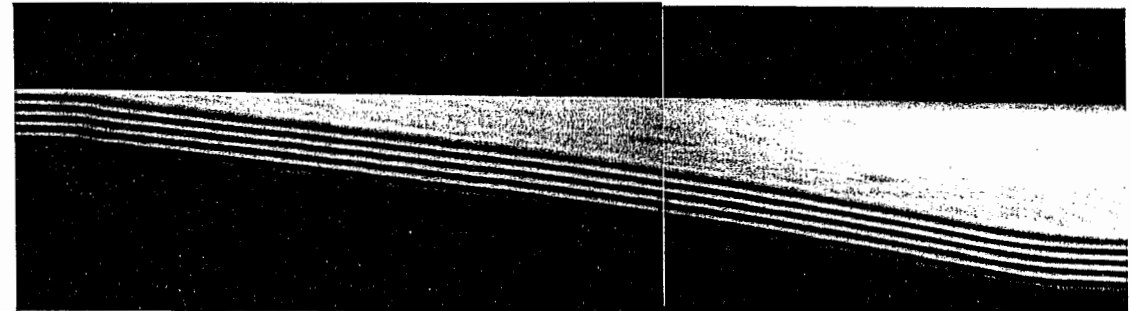
0.2 μm GaAs

1 μm

(g) $\theta = 13^\circ / (014)$



(h) $\theta = 9^\circ / (016)$



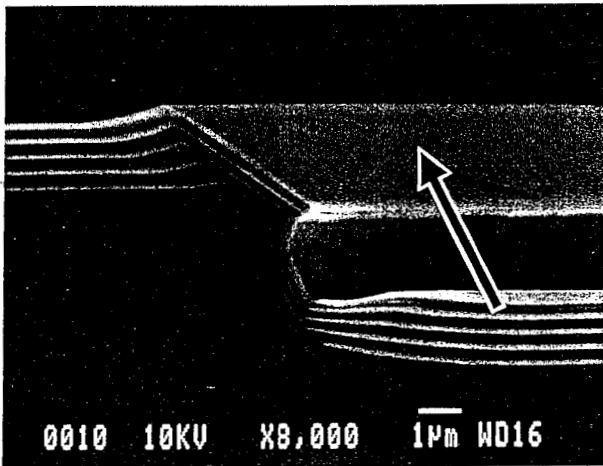
0.2 μm Al_{0.3}Ga_{0.7}As

Figure 11 (110) cross-sectional views of the after-growth profiles of the (010)-related sidewalls corresponding to Figure 10.

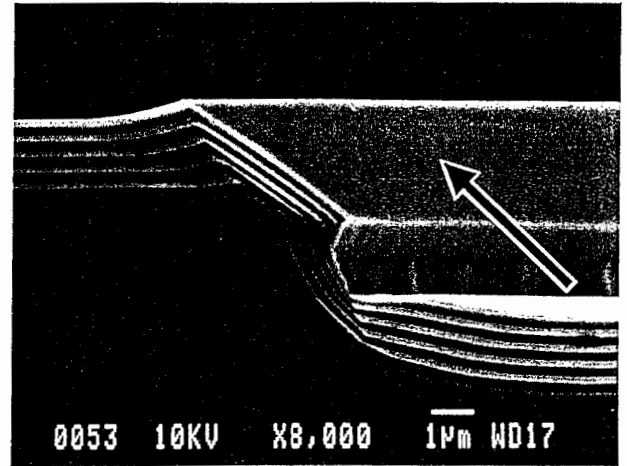
—30—

(011) / $\theta_f = 45^\circ$

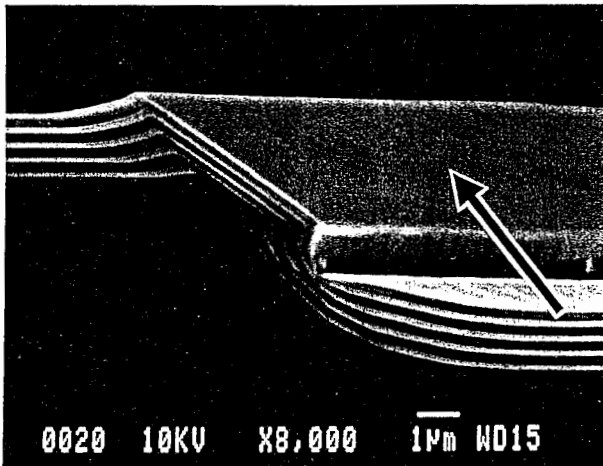
(a) $\theta = 89^\circ / (010)$



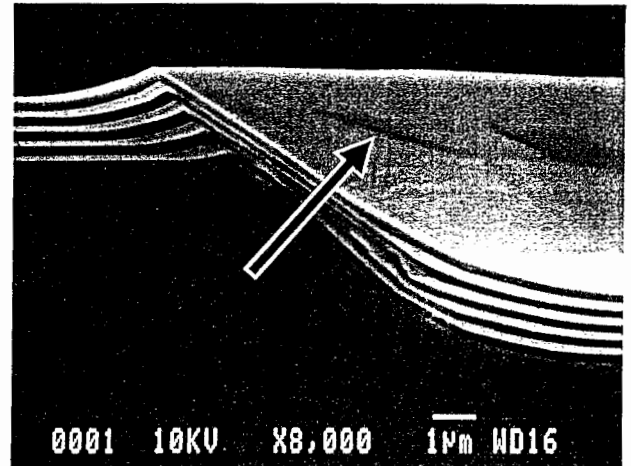
(b) $\theta = 83^\circ / (081)$



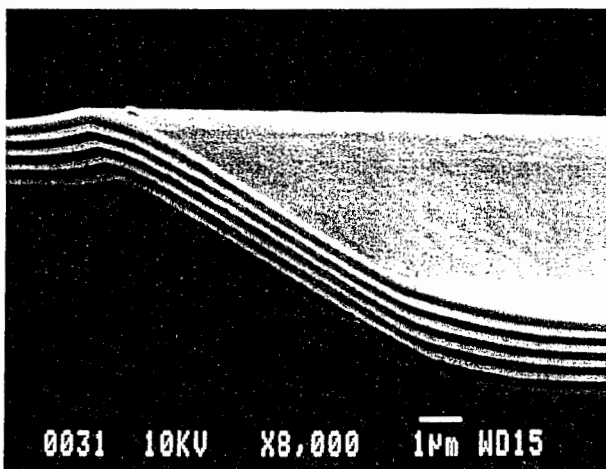
(c) $\theta = 71^\circ / (031)$



(d) $\theta = 47^\circ / (098)$



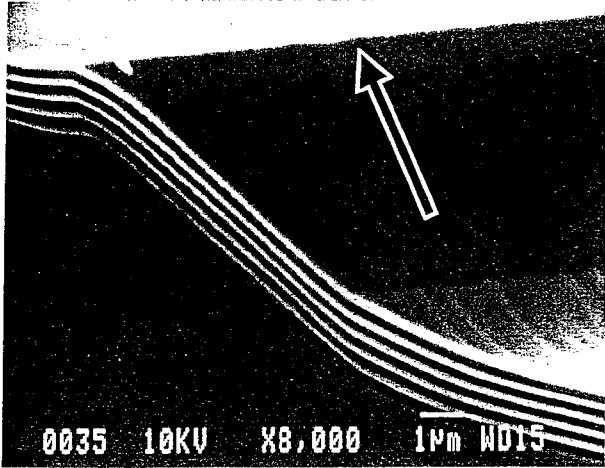
(e) $\theta = 43^\circ / (089)$



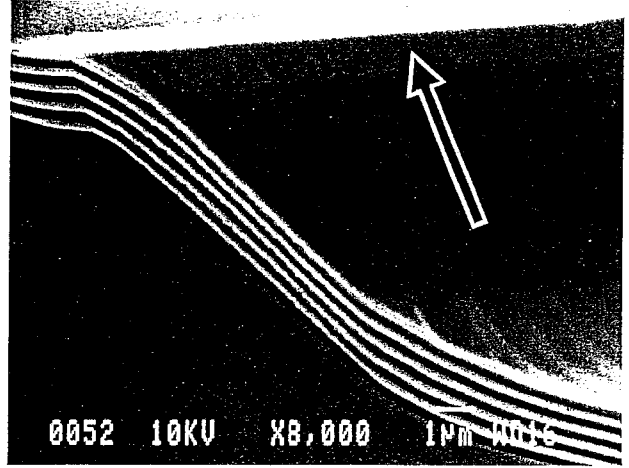
Figures 12 Bird's eye views of the growth behavior of the (011) facet (indicated by arrow) with respect to θ .

(013) / $\theta_f = 19^\circ$

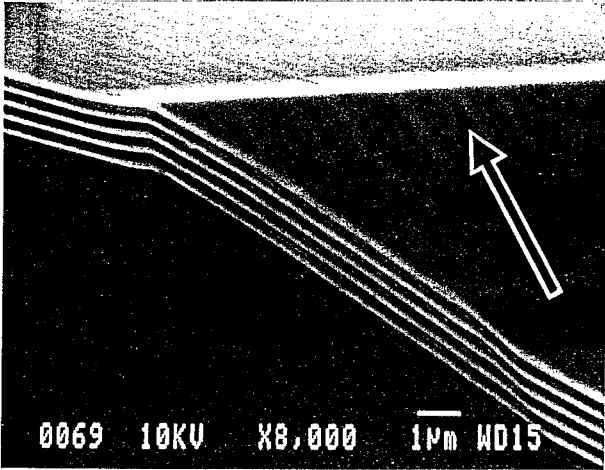
(a) $\theta = 43^\circ / (089)$



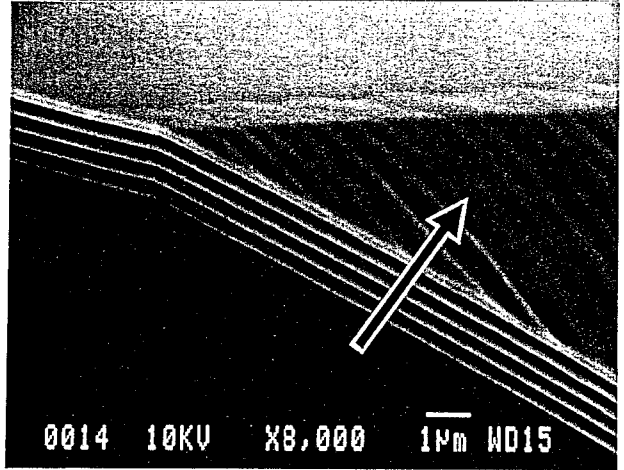
(b) $\theta = 39^\circ / (045)$



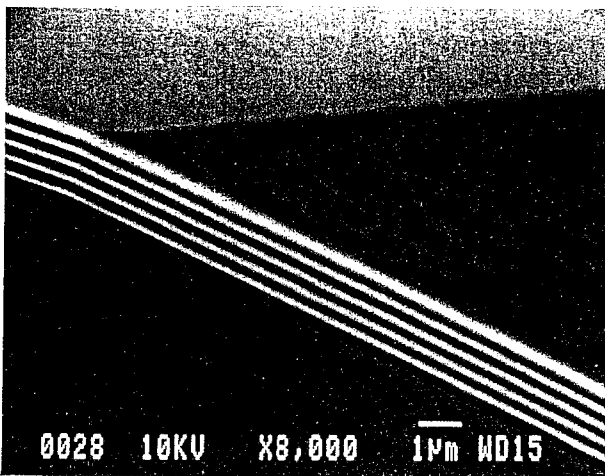
(c) $\theta = 28^\circ / (012)$



(d) $\theta = 21^\circ / (025)$



(e) $\theta = 13^\circ / (014)$



Figures 13 Bird's eye views of the growth behavior of the (013) facet (indicated by arrow) with respect to θ .

HF : H₂O₂ : H₂O = x : y : z

at 25 °C

x = 0.05 mol / y = 0.04 - 0.34 mol / z = 1.22 - 56.82 mol

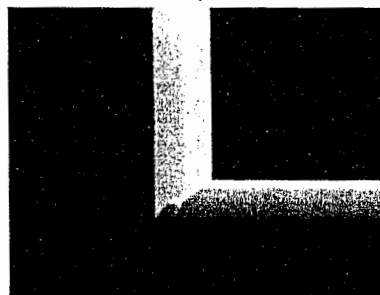
(a) $\theta = 54^\circ / (111)A^1; \theta = 57^\circ / (\bar{9}98)B^2$



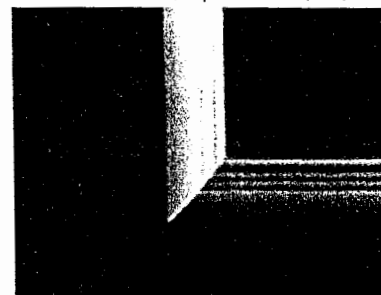
(b) $\theta = 51^\circ / (889)A; \theta = 54^\circ / (\bar{1}11)B$



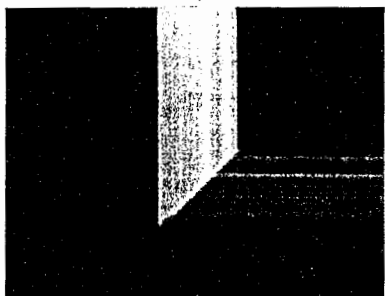
(c) $\theta = 50^\circ / (667)A; \theta = 52^\circ / (\bar{8}89)B$



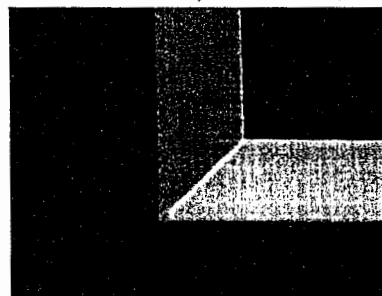
(d) $\theta = 49^\circ / (445)A; \theta = 47^\circ / (\bar{3}34)B$



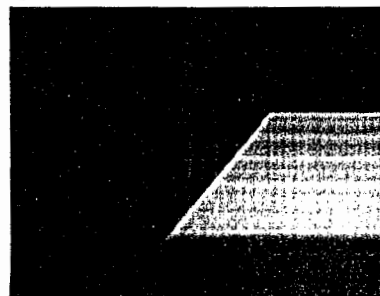
(e) $\theta = 41^\circ / (335)A; \theta = 40^\circ / (\bar{3}35)B$



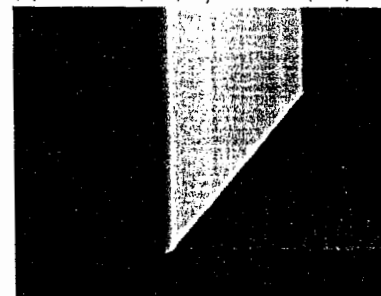
(f) $\theta = 37^\circ / (112)A; \theta = 36^\circ / (\bar{1}12)B$



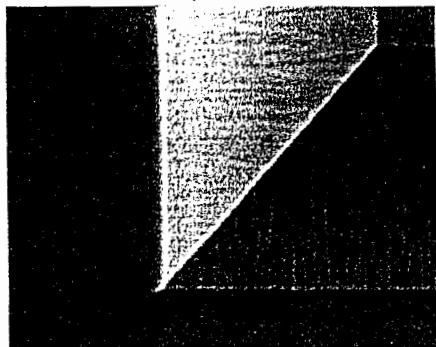
(g) $\theta = 32^\circ / (449)A; \theta = 26^\circ / (\bar{1}13)B$



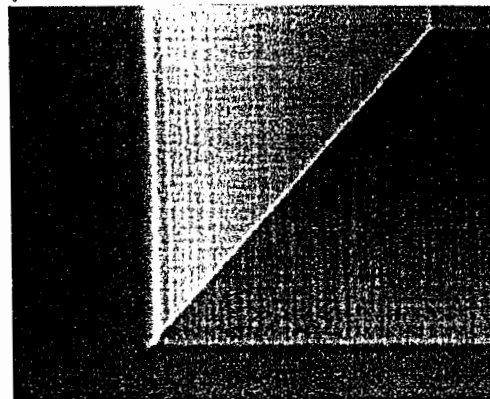
(h) $\theta = 24^\circ / (113)A; \theta = 20^\circ / (\bar{1}14)B$



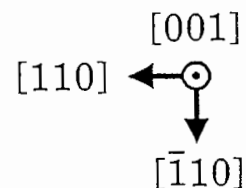
(i) $\theta = 13^\circ / (116)A; \theta = 12^\circ / (\bar{1}17)B$



(j) $\theta = 9^\circ / (119)A; \theta = 9^\circ / (\bar{1}19)B$



10 μm



1) $[\bar{1}10]$ stripe 2) $[110]$ stripe

Figure 14 Top views of the as-etched profiles of the intersections of the $[\bar{1}10]$ and $[110]$ stripes with various sidewall slopes.

Growth temperature = 620 °C

V/III flux ratio = 7.4 (GaAs) / 6.2 (Al_{0.3}Ga_{0.7}As)

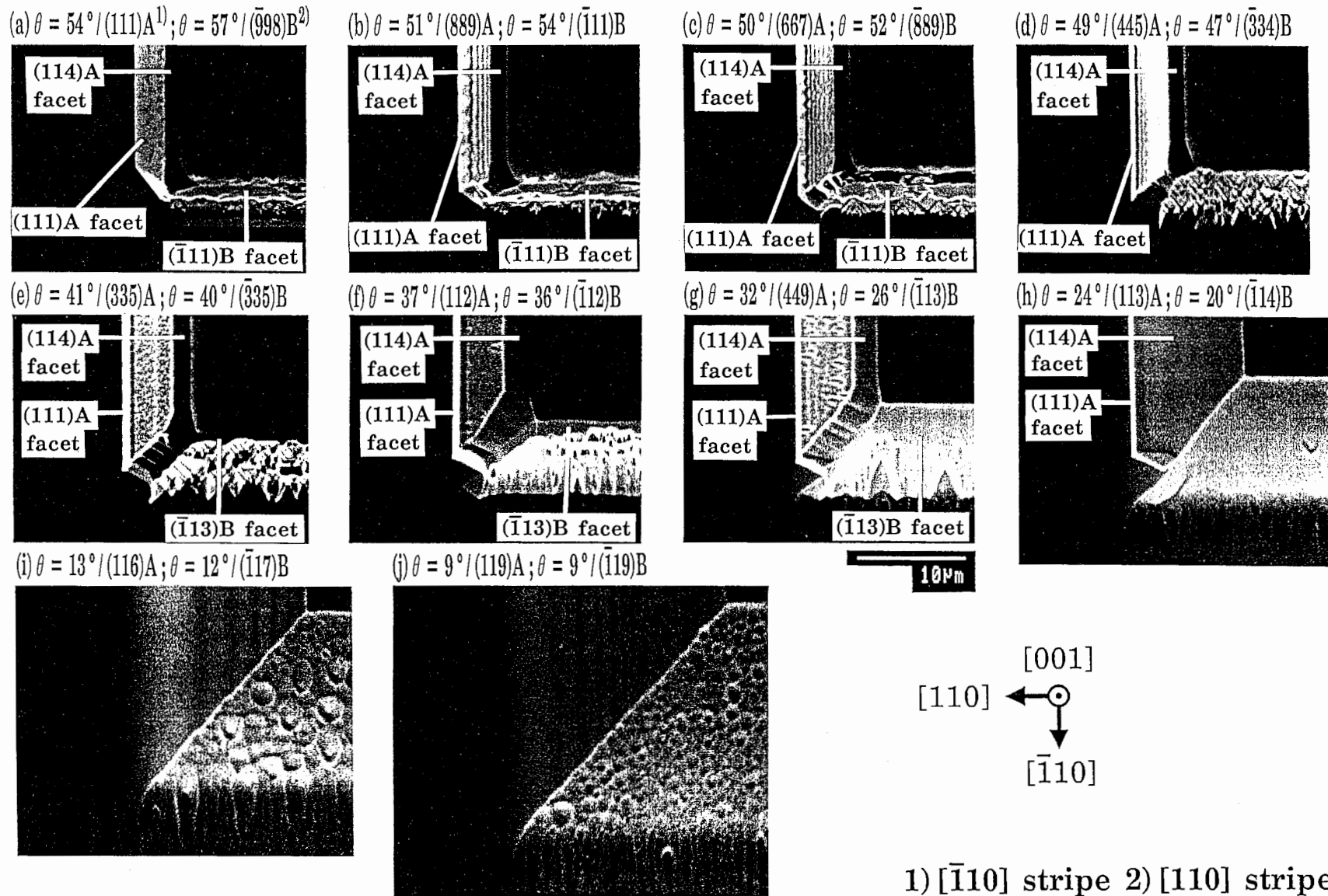


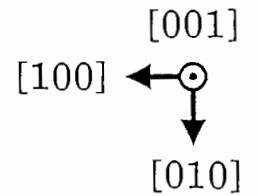
Figure 15 Top views of the after-growth profiles of the intersections of the $[\bar{1}10]$ and $[110]$ stripes corresponding to Figure 14.

—34—

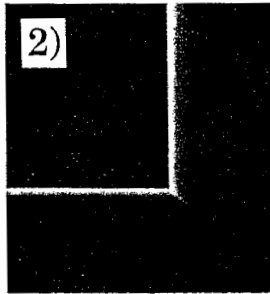
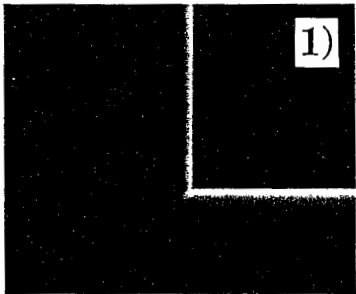
HF: H₂O₂: H₂O = x: y: z at 25 °C

x = 0.05 mol / y = 0.04 - 0.34 mol / z = 1.22 - 56.82 mol

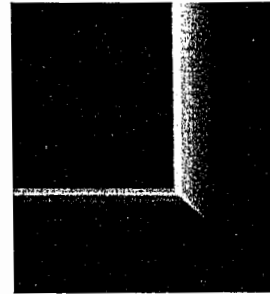
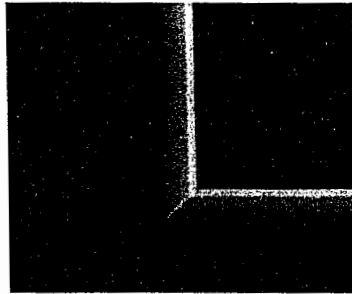
1) (111)A-related corner
2) ($\bar{1}\bar{1}\bar{1}$)B-related corner



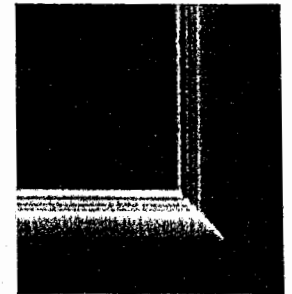
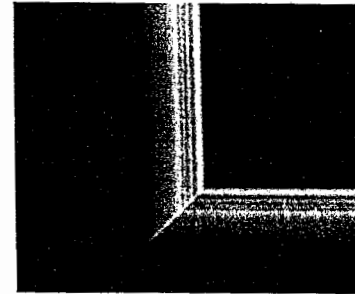
(a) $\theta = 89^\circ / (100)$



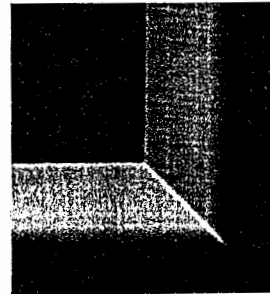
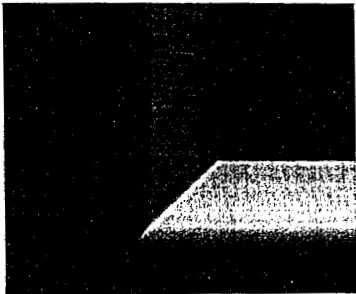
(b) $\theta = 71^\circ / (301)$



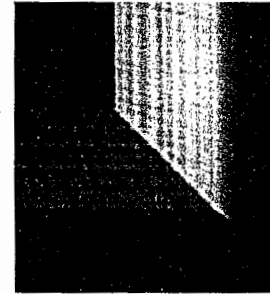
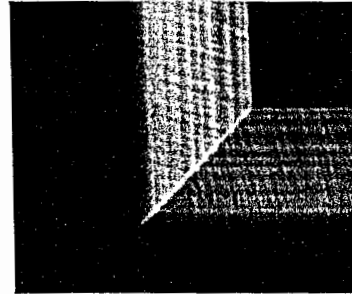
(c) $\theta = 47^\circ / (908)$



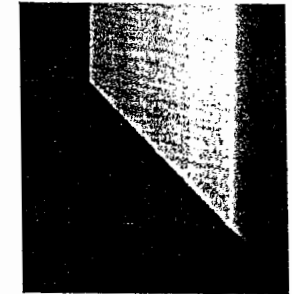
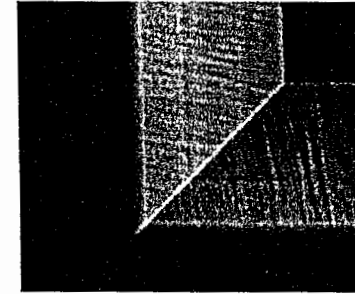
(d) $\theta = 39^\circ / (405)$



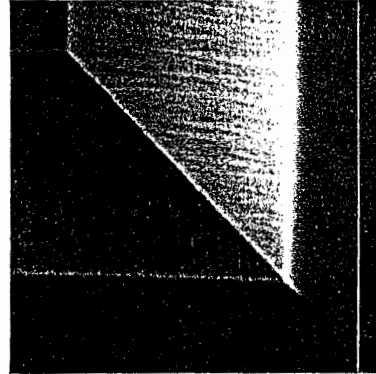
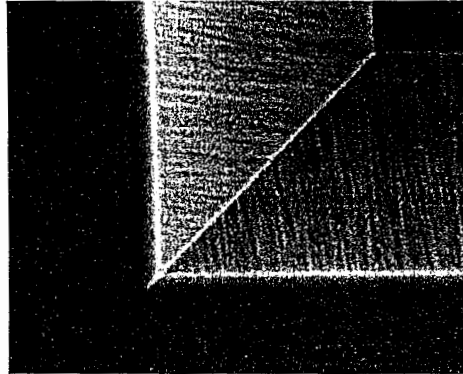
(e) $\theta = 28^\circ / (102)$



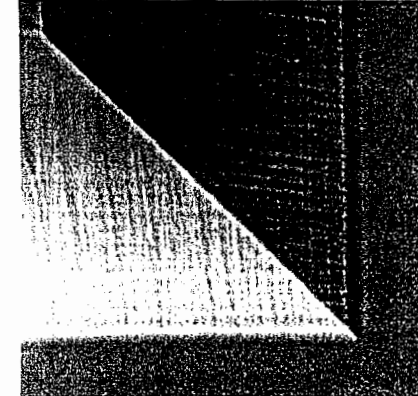
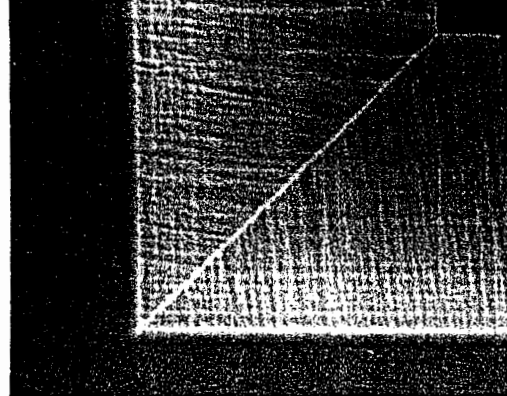
(f) $\theta = 21^\circ / (205)$



(g) $\theta = 13^\circ / (104)$



(h) $\theta = 9^\circ / (106)$



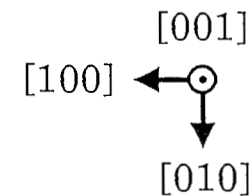
10µm

Figure 16 Top views of the as-etched profiles of the intersections of the [100] and [010] stripes with various sidewall slopes.

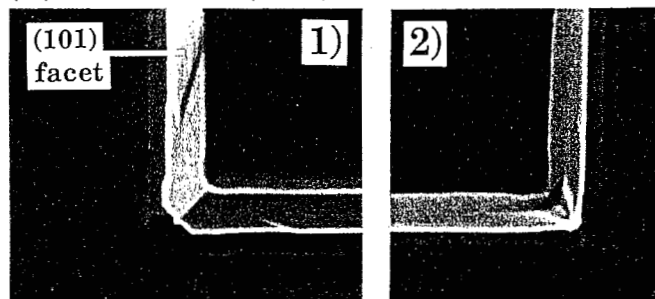
Growth temperature = 620 °C

V/III flux ratio = 7.4 (GaAs) / 6.2 (Al_{0.3}Ga_{0.7}As)

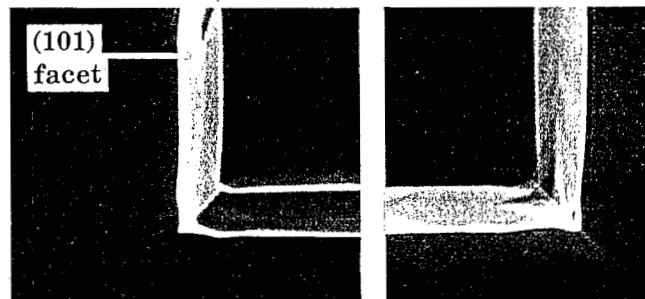
1) (111)A-related corner
2) ($\bar{1}\bar{1}\bar{1}$)B-related corner



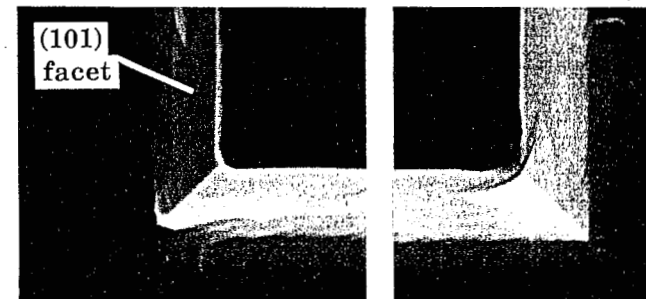
(a) $\theta = 89^\circ / (100)$



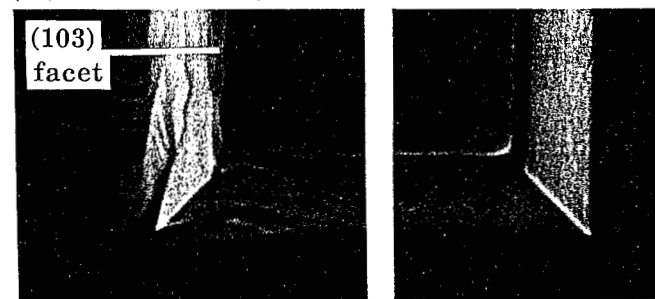
(b) $\theta = 71^\circ / (301)$



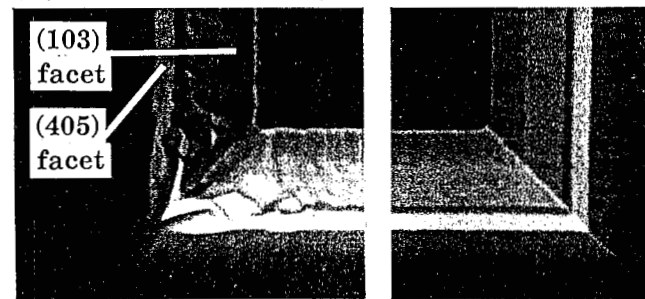
(c) $\theta = 47^\circ / (908)$



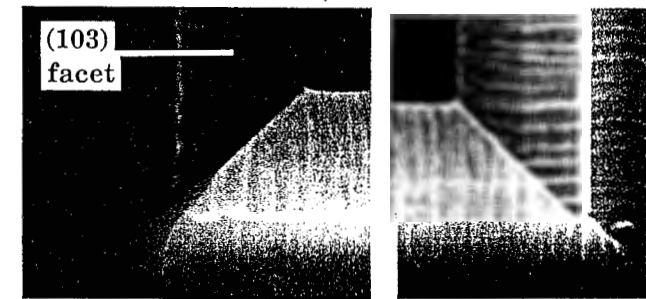
(d) $\theta = 39^\circ / (405)$



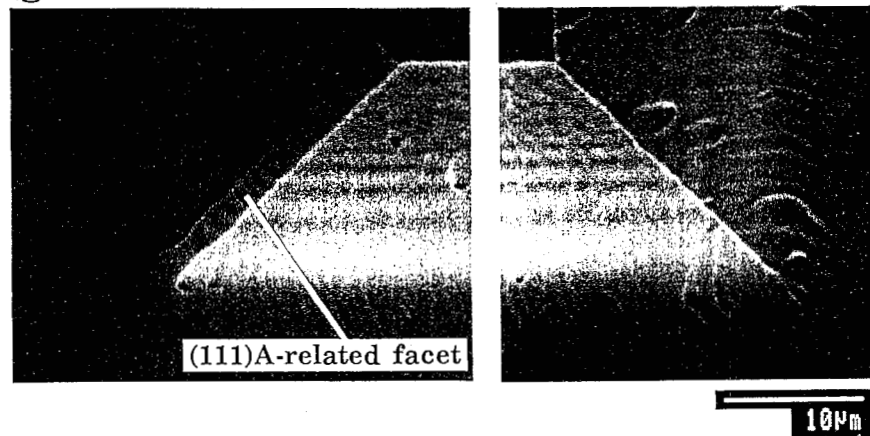
(e) $\theta = 28^\circ / (102)$



(f) $\theta = 21^\circ / (205)$



(g) $\theta = 13^\circ / (104)$



(h) $\theta = 9^\circ / (106)$

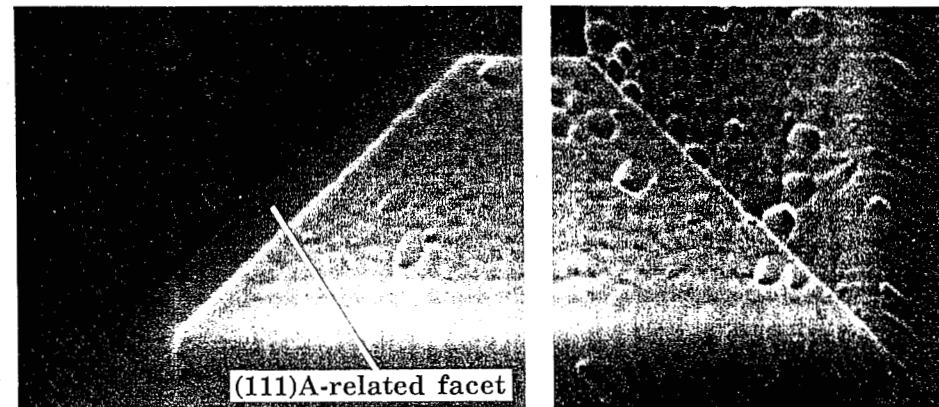


Figure 17 Top views of the after-growth profiles of the intersections of the [100] and [010] stripes corresponding to Figure 16.

Substrate	Sidewall slope	Extra facet on sidewall		Extra facet on corner	
		Slope	Orientation	Slope	Orientation
(001)	$[\bar{1}10]$ stripe	55°	(111)A	/	/
	$\geq 21^\circ$	21°	(114)A		
	$< 21^\circ$	No facets			
	$[110]$ stripe	Slope	Orientation	Slope	Orientation
	$\geq 53^\circ$	53°	($\bar{1}11$)B	/	/
	$53^\circ \sim 24^\circ$	24°	($\bar{1}13$)B		
	$< 24^\circ$	No facets			
	$[100]$ stripe	Slope	Orientation	Slope	Orientation
	$\geq 45^\circ$	72°	(031)	No facets	
		45°	(011)		
	$45^\circ \sim 19^\circ$	38°	(045)	No facets	
		19°	(013)		
	$< 19^\circ$	No facets		$\leq 13^\circ$	(116)A etc.

Table 1 Summary of facet generation behavior during MBE on GaAs (001) patterned substrates.